Electronic Supplementary Information for CrystEngComm
This journal is © The Royal Society of Chemistry 2017

Supporting Information For

A cerium-based metal-organic framework having inherent oxidase-like activity applicable for colorimetric sensing of biothiols and aerobic oxidation of thiols

Rana Dalapati,[a] *Balasubramanian Sakthivel,*[b] *Manoj K. Ghosalya,*[c] *Amarajothi Dhakshinamoorthy,*[b] and Shyam Biswas*[a]*

[a] Department of Chemistry, Indian Institute of Technology Guwahati, Guwahati, 781039 Assam, India

[b] School of Chemistry, Madurai Kamaraj University, 625021 Madurai, Tamil Nadu, India

[c] Catalysis Division, National Chemical Laboratory, Dr. Homi Bhabha Road, Pune 411008, India

* To whom correspondence should be addressed. E-mail: sbiswas@iitg.ernet.in; admguru@gmail.com.

Table S1. Refined unit cell parameters for as-synthesized **1** and isostructural Zr(IV)-based compound having cubic unit cells.

Compound	*a* (Å)	*V* (Å^3)
as-synthesized **1**	23.111(6)	12343.6(54)
$[Zr_6O_4(OH)_4(DMTDC)_6]\cdot 4.8DMF\cdot 10H_2O$ [1]	23.0917(6)	12313.1(3)
Zr-DMTDC [2]	23.12	12358.43

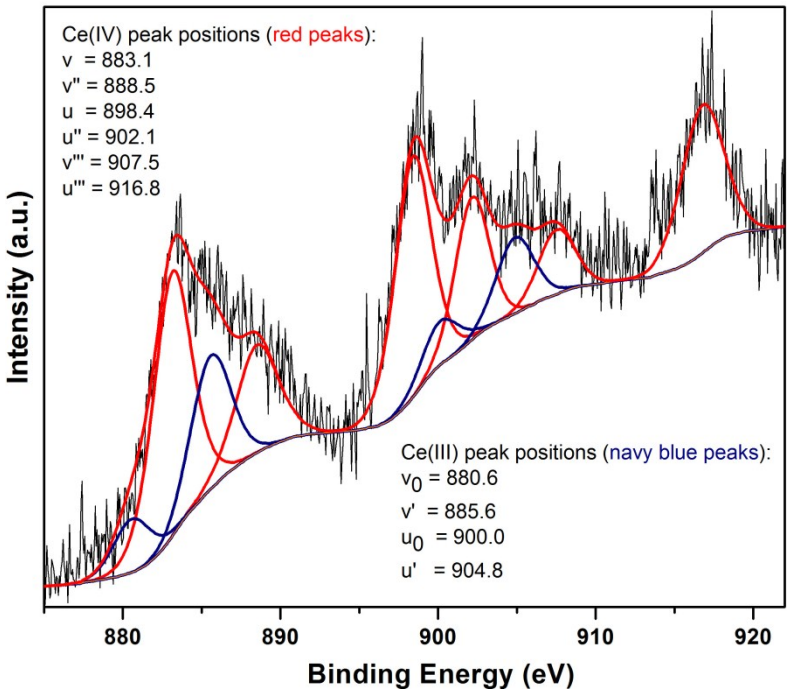

Figure S1. XPS spectrum of the as-synthesized form of **1** (Ce 3d core level).

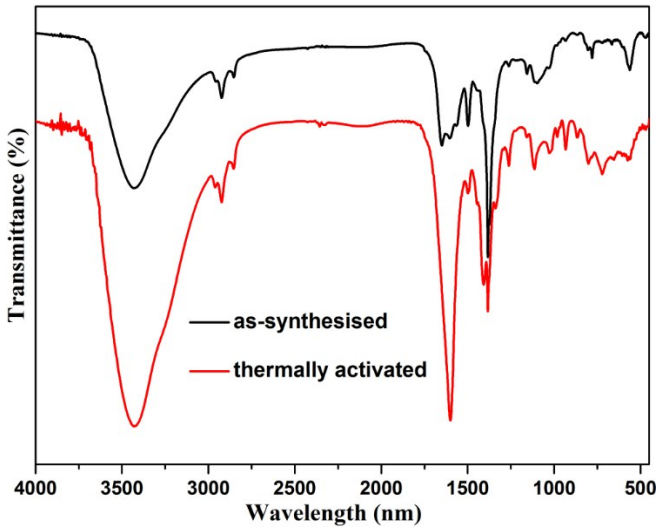

Figure S2. FT-IR spectra of the as-synthesized (black) and thermally activated (red) forms of **1**.

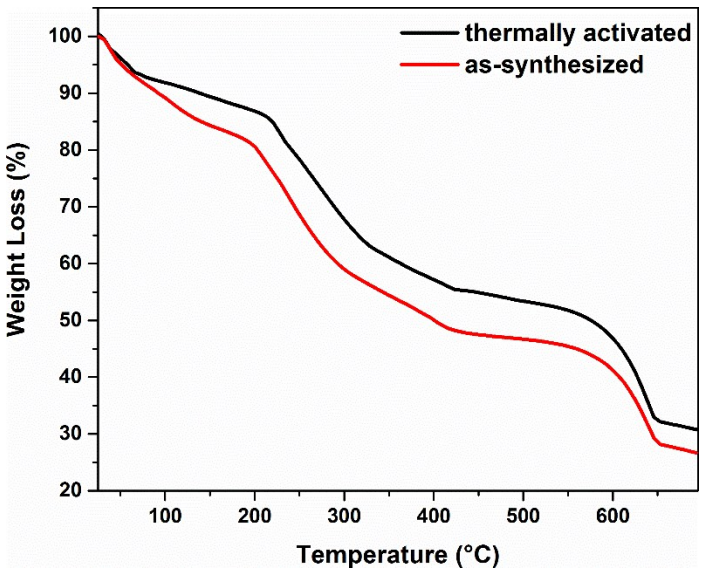

Figure S3. TG curves of as-synthesized (red) and thermally activated (black) forms of **1** measured under air atmosphere in the range 25-700 ˚C at a heating rate of 5 °C min^{-1}.

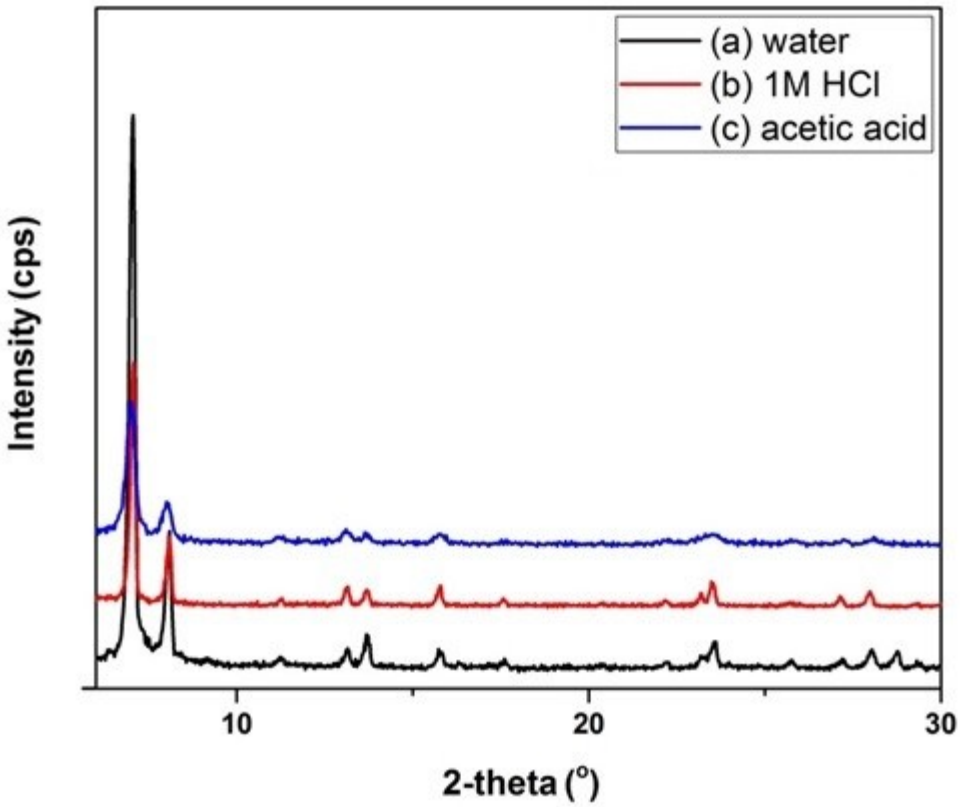

Figure S4. XRPD patterns of **1'** after treatment with (a) water, (b) 1M HCl and (c) acetic acid.

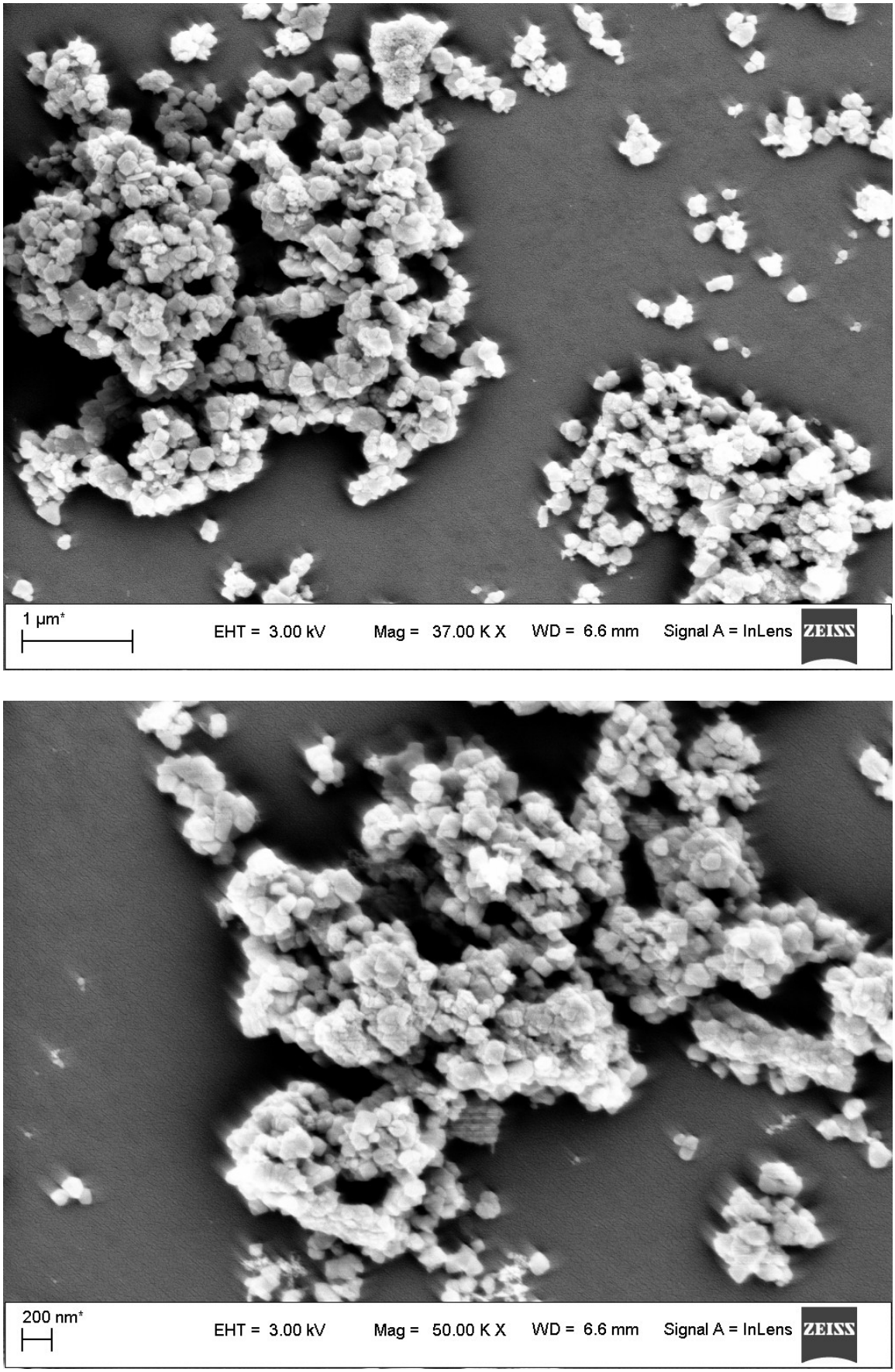

Figure S5. FE-SEM images of activated **1'**.

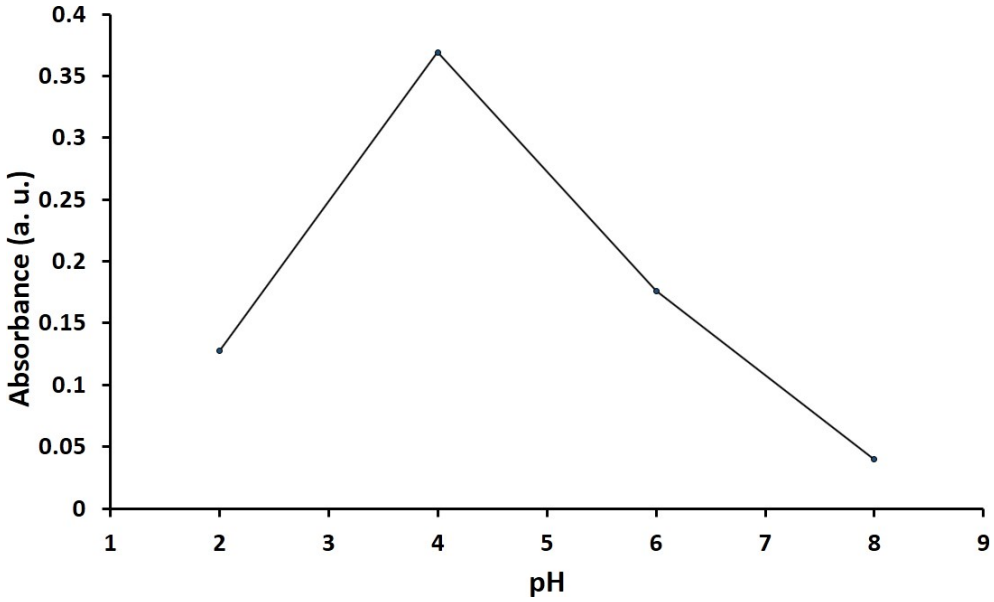

Figure S6. Effect of pH on the oxidase-like catalytic activity of **1'** towards TMB.

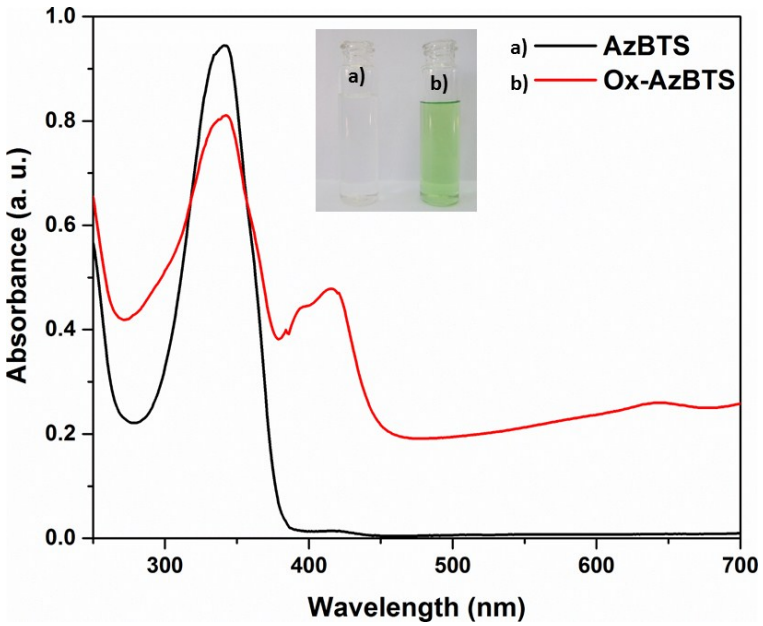

Figure S7. UV-vis absorption spectra of AzBTS in the absence (black) and presence (red) of **1'**. Inset: digital photographs of vials containing AzBTS in the absence (a) and presence (b) of **1'**.

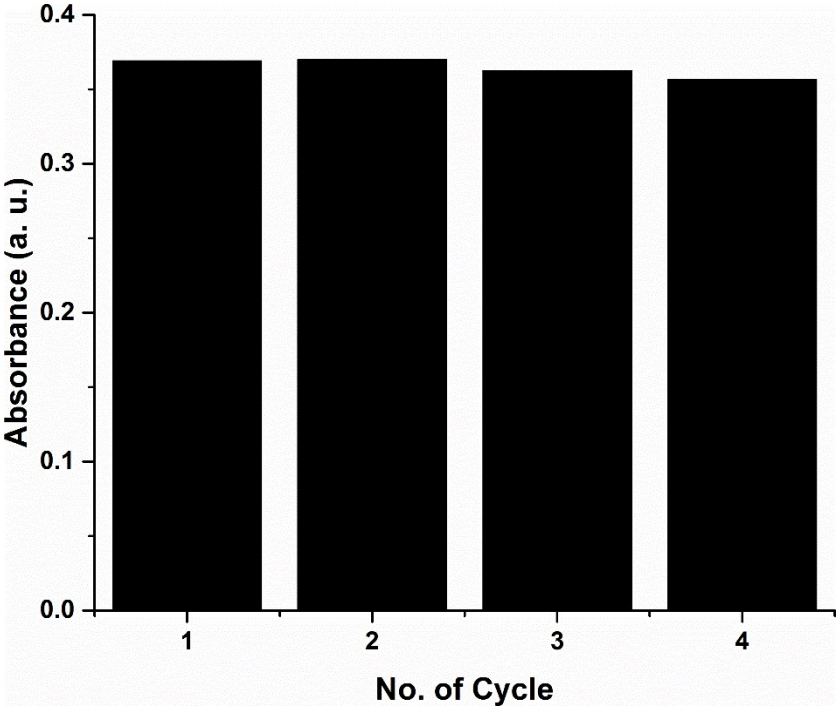

Figure S8. Recyclability of the oxidase-like catalytic activity of **1'** towards TMB.

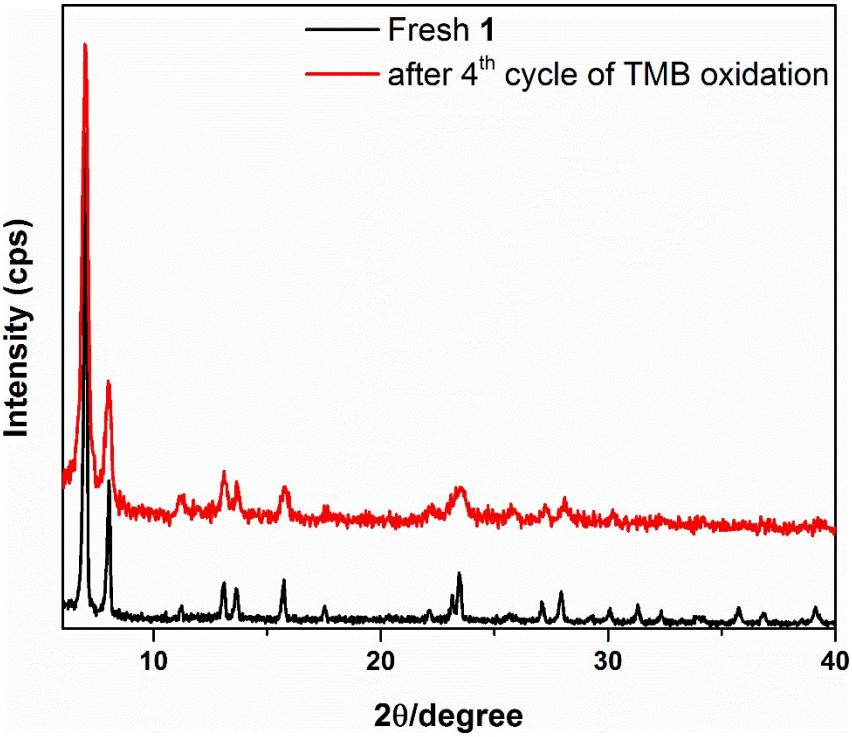

Figure S9. XRPD patterns of **1'** before and after oxidase-like catalytic activity towards TMB.

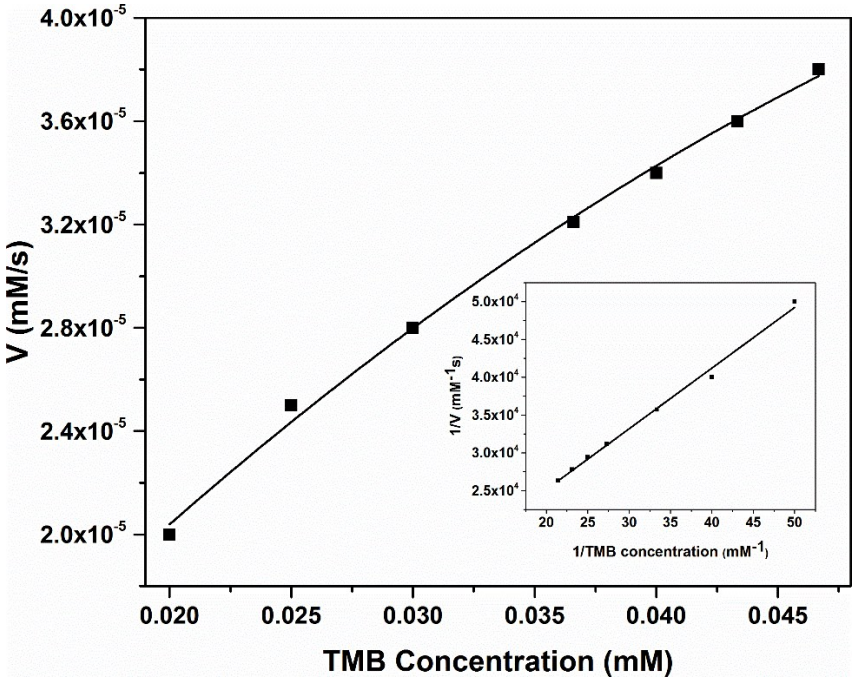

Figure S10. Steady-state kinetic assay of **1'** with TMB at pH = 4. Inset: Lineweaver–Burk plot of the double reciprocal of the Michaelis–Menten equation.

Table S2. Comparison of the kinetic parameters of different nano-enzymes that mimic peroxidase/oxidase at pH = 4.

Sl. No.	Nano-enzyme	K_m (mM)	V_{max} (M s^{-1})	Ref.
1.	Ce-DMTDC (**1'**)	0.088	0.11×10^{-6}	This work
2.	HRP	0.43	10.0×10^{-8}	[3]
3.	isPNC (nanoceria)	3.8	0.7×10^{-6}	[4]
4.	swPNC (nanoceria)	1.9	0.6×10^{-6}	
5.	isDNC (nanoceria)	1.8	0.5×10^{-6}	
6.	swDNC (nanoceria)	0.8	0.3×10^{-6}	
7.	MIL-53(Fe)	1.08	8.78×10^{-8}	[5]
8.	JFSNs	3.05	4.16×10^{-6}	[6]
9.	Fe_3O_4@C	0.38	73.99×10^{-8}	[7]
10.	Ce-MOF (MVCM)	0.37	5.5×10^{-6}	[8]
11.	CuNPs@C	1.65	12.05×10^{-8}	[9]
12.	Fe-MIL-88NH_2	0.284	10.47×10^{-8}	[10]
13.	hemin@MIL-53(Al)-	0.068	6.07×10^{-8}	[11]

	NH_2			
14.	MIL-53(Fe) by MW	0.28	4.48×10^{-8}	[12]
15.	Fe-MIL-101-FA	0.164	1.55×10^{-8}	[13]

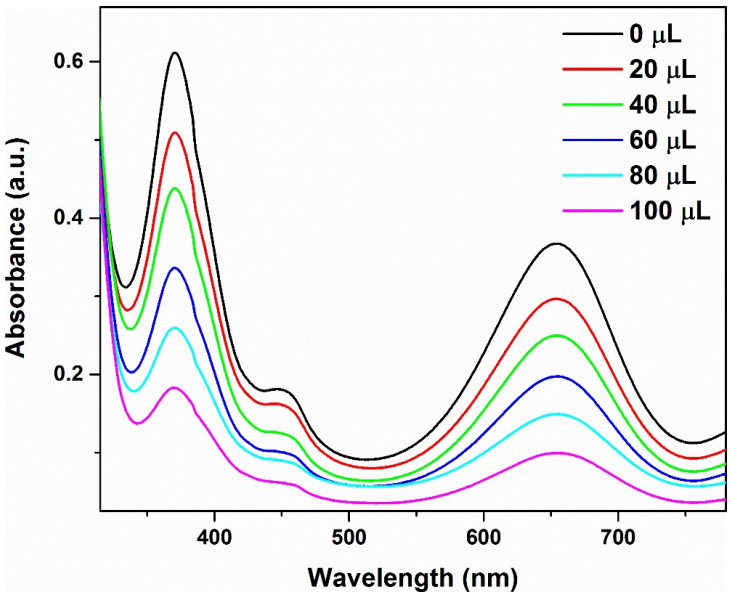

Figure S11. Absorbance spectra of ox-TMB in presence of glutathione at varying concentration.

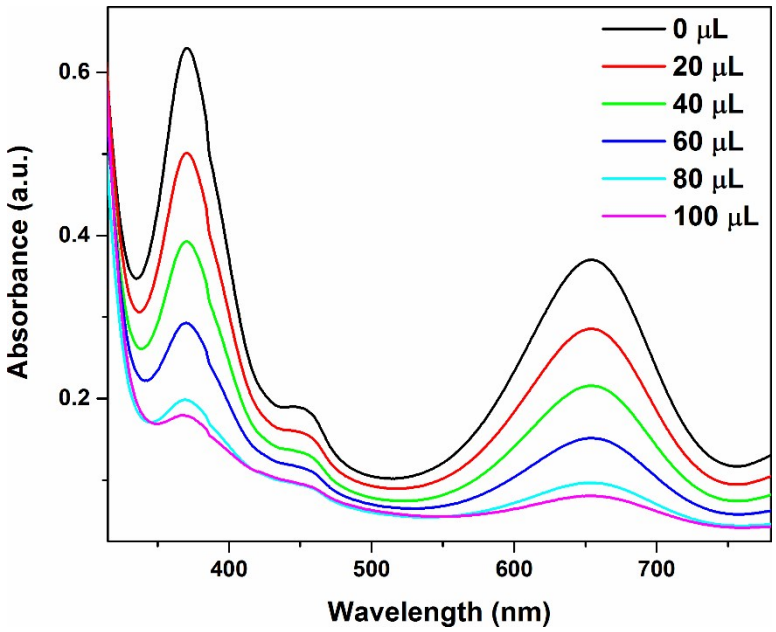

Figure S12. Absorbance spectra of ox-TMB in presence of homocysteine at varying concentration.

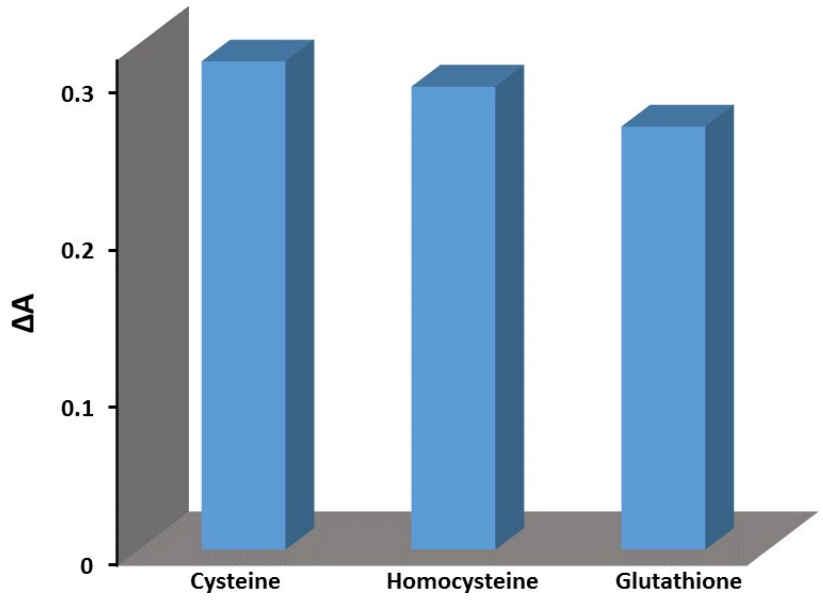

Figure S13. Change in the absorbance of ox-TMB in presence of different biothiols.

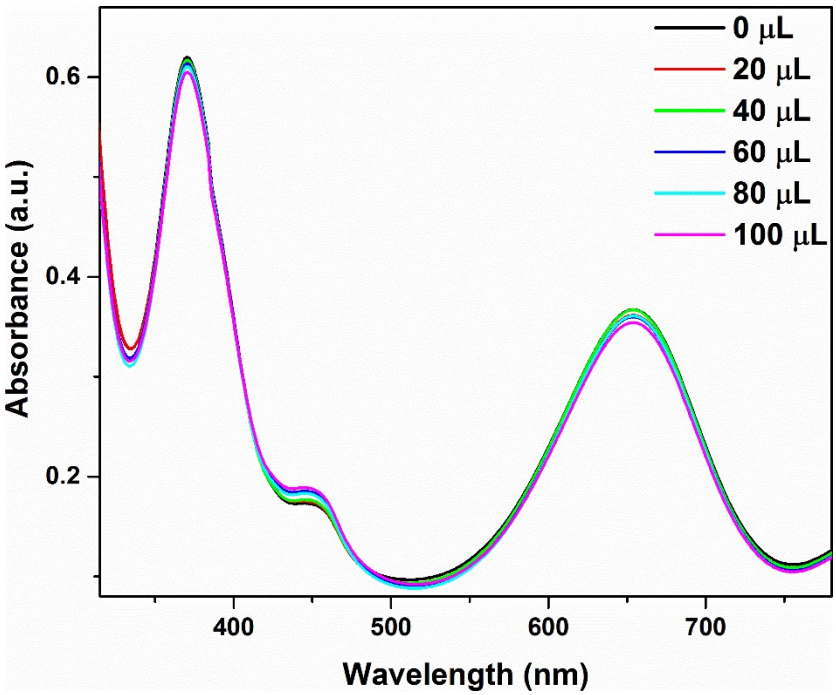

Figure S14. UV-vis absorption spectra of ox-TMB in presence of various concentrations of alanine.

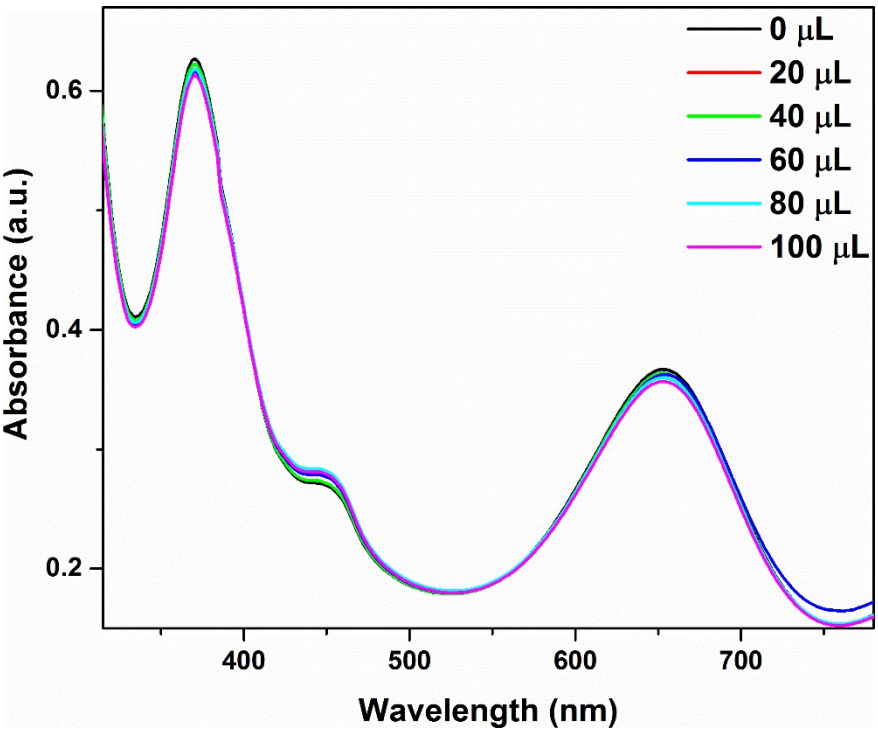

Figure S15. UV-vis absorption spectra of ox-TMB in presence of various concentrations of arginine.

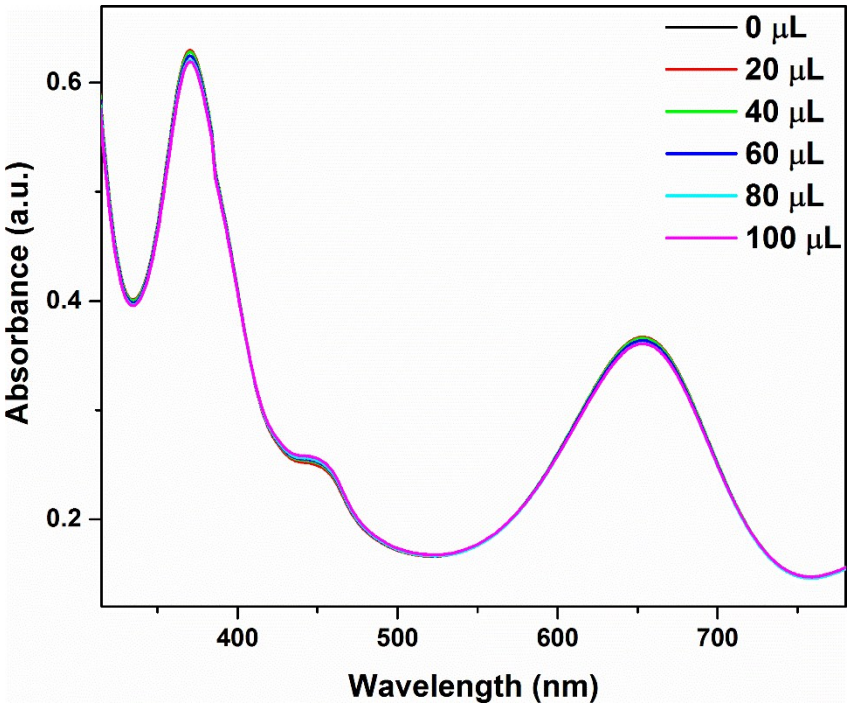

Figure S16. UV-vis absorption spectra of ox-TMB in presence of various concentrations of aspartic acid.

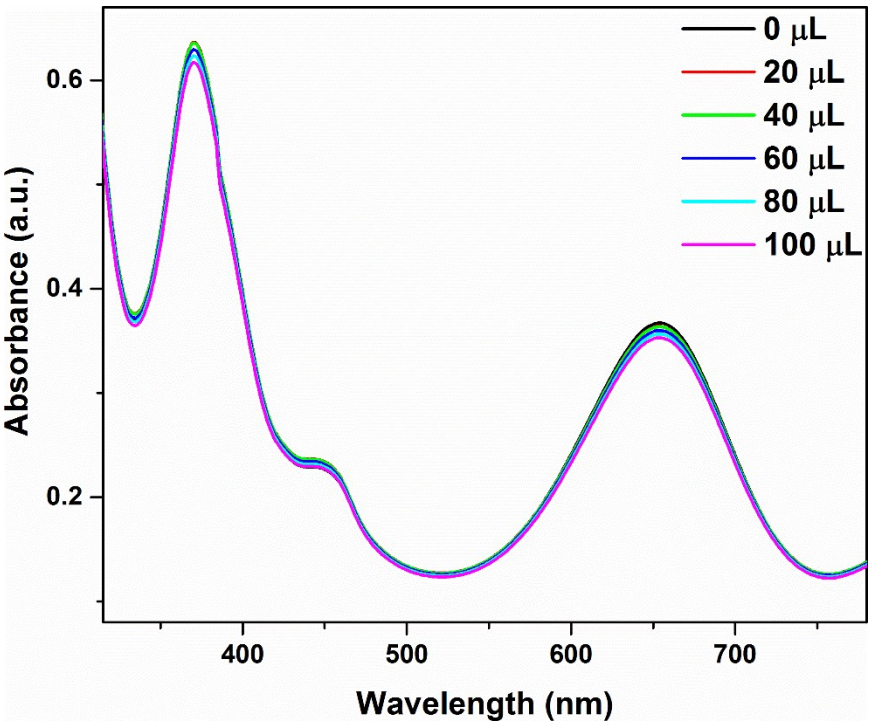

Figure S17. UV-vis absorption spectra of ox-TMB in presence of various concentrations of glycine.

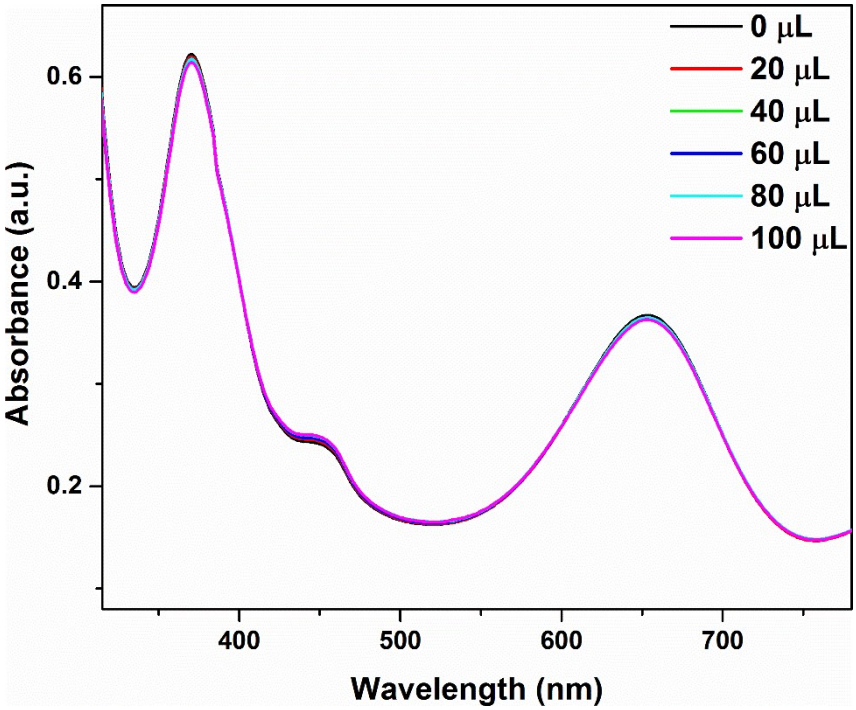

Figure S18. UV-vis absorption spectra of ox-TMB in presence of various concentrations of histidine.

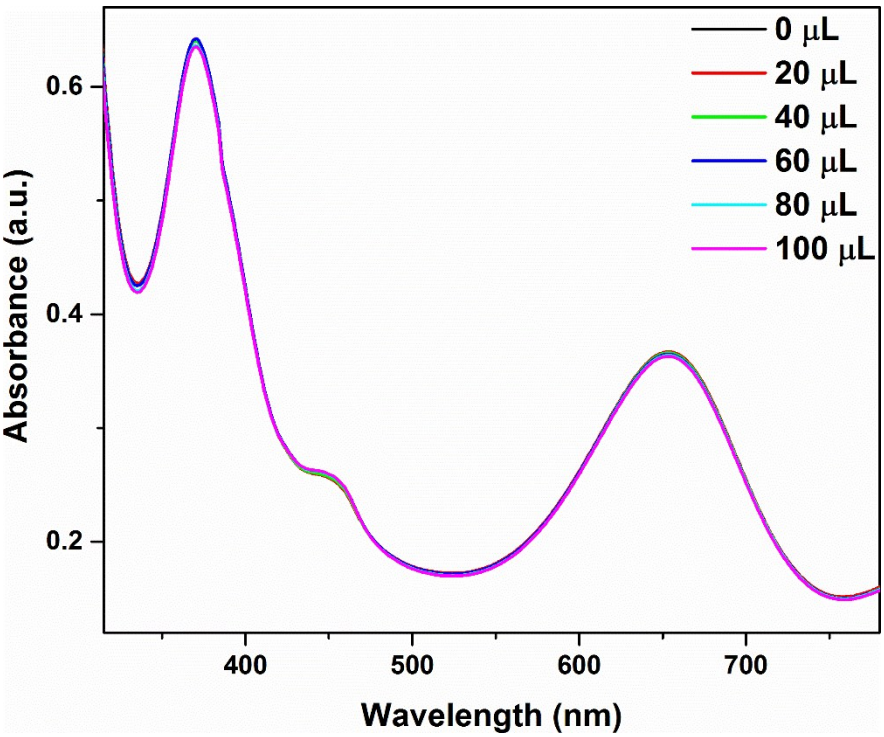

Figure S19. UV-vis absorption spectra of ox-TMB in presence of various concentrations of isoleucine.

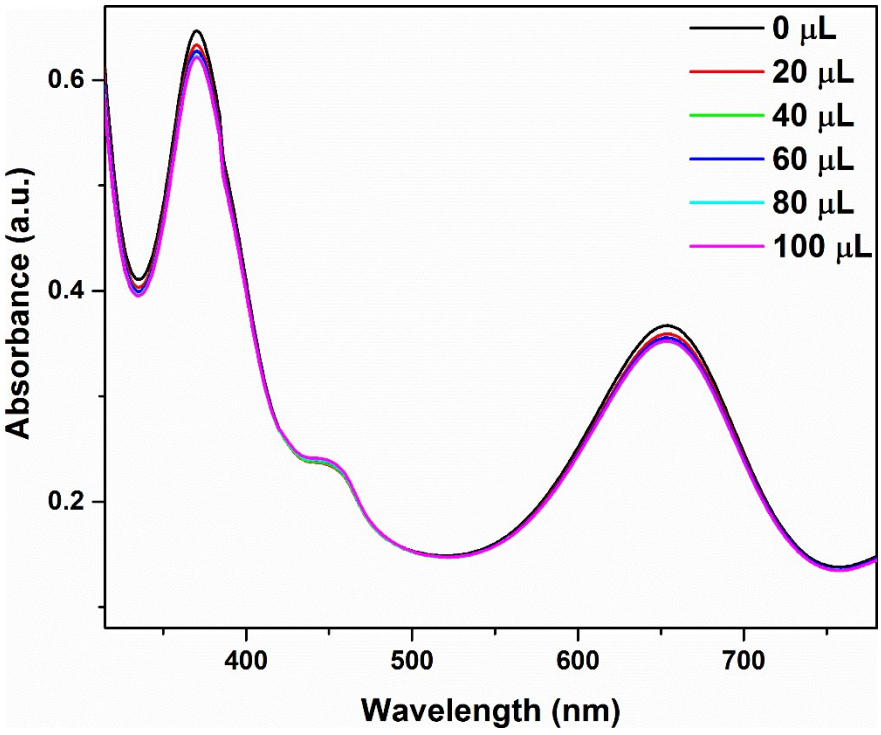

Figure S20. UV-vis absorption spectra of ox-TMB in presence of various concentrations of leucine.

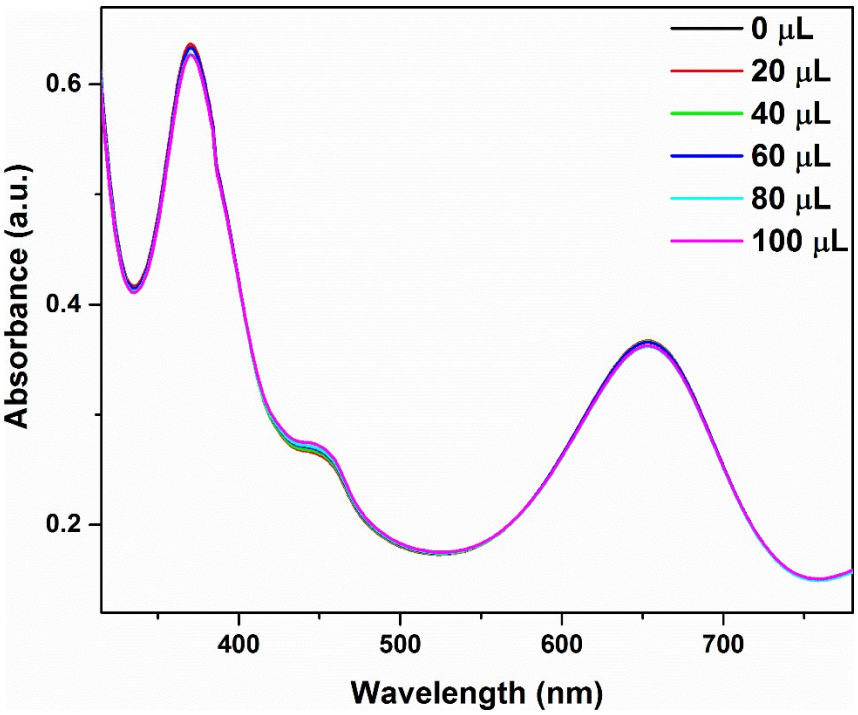

Figure S21. UV-vis absorption spectra of ox-TMB in presence of various concentrations of lysine.

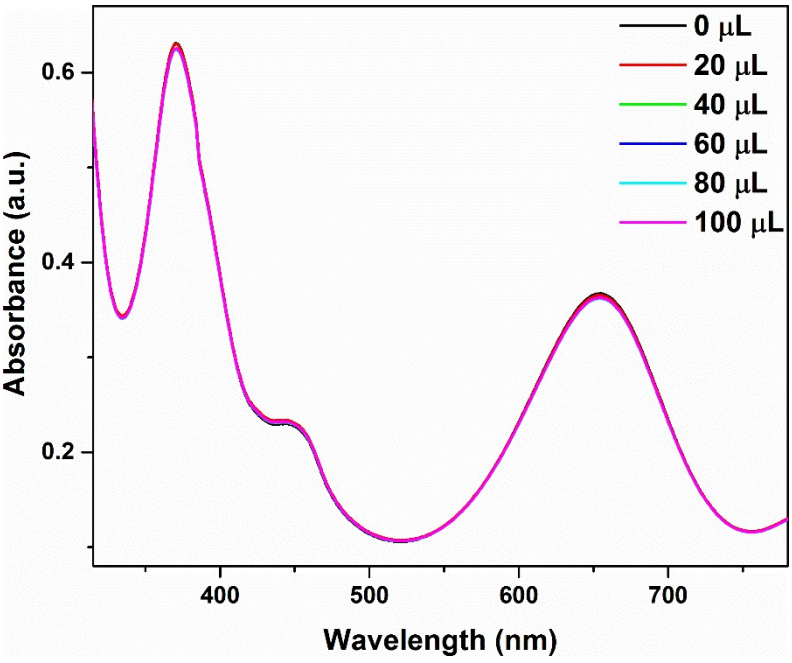

Figure S22. UV-vis absorption spectra of ox-TMB in presence of various concentrations of methionine.

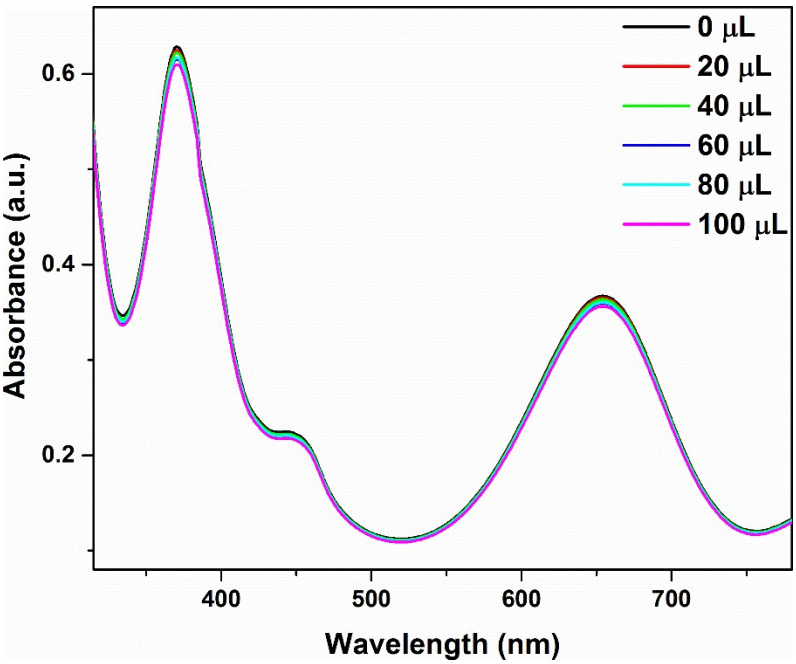

Figure S23. UV-vis absorption spectra of ox-TMB in presence of various concentrations of phenyl alanine.

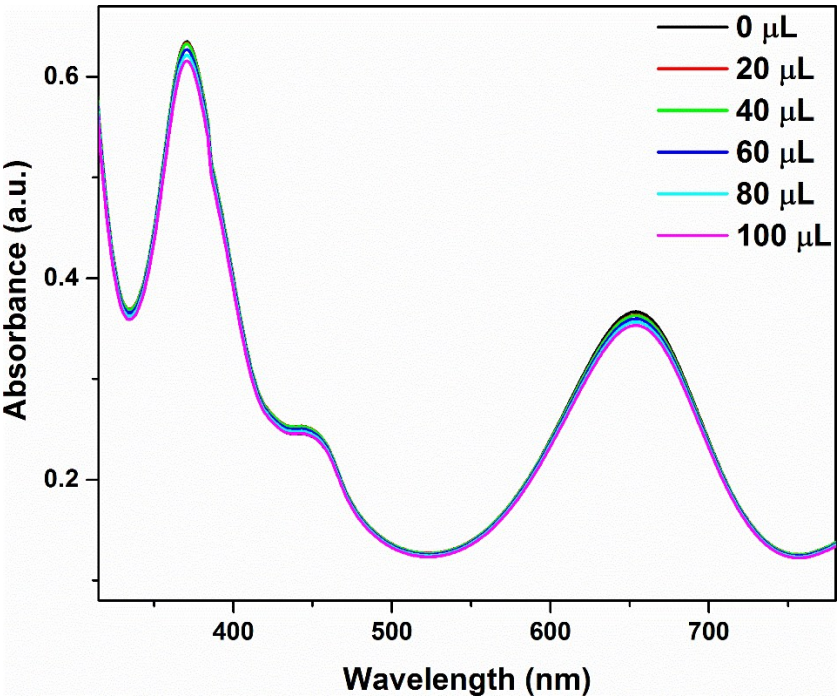

Figure S24. UV-vis absorption spectra of ox-TMB in presence of various concentrations of proline.

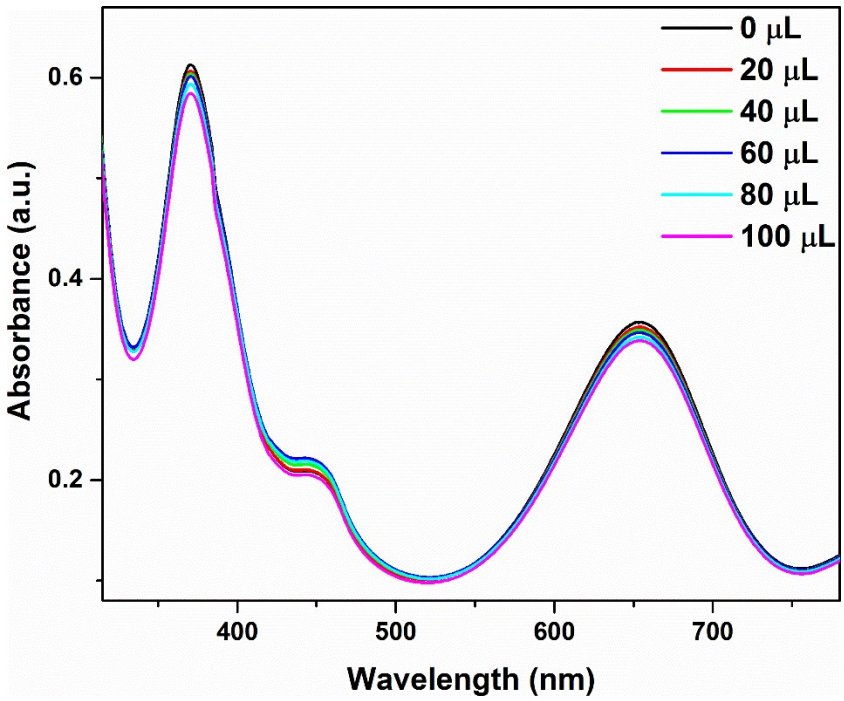

Figure S25. UV-vis absorption spectra of ox-TMB in presence of various concentrations of serine.

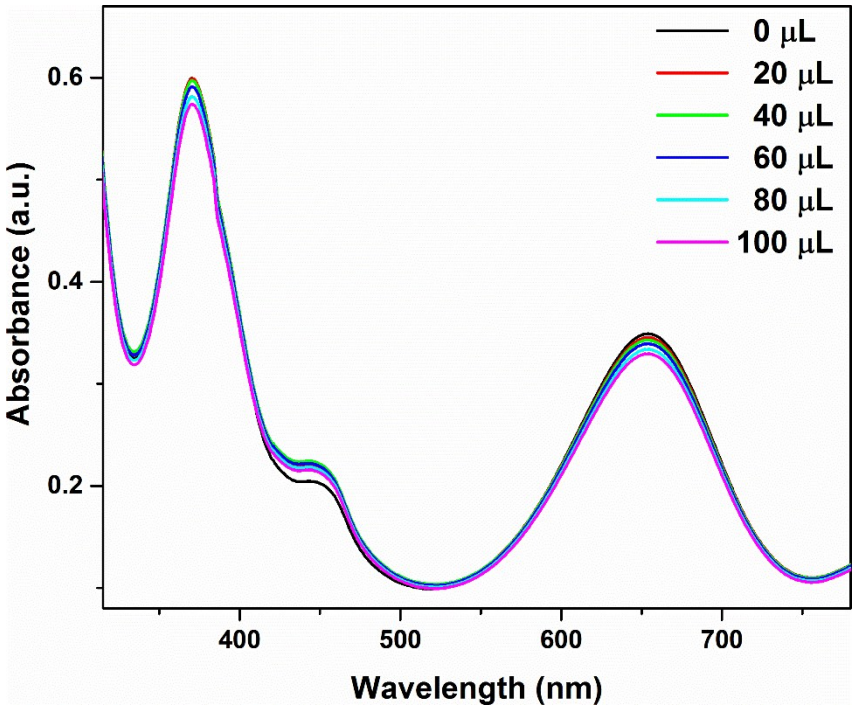

Figure S26. UV-vis absorption spectra of ox-TMB in presence of various concentrations of threonine.

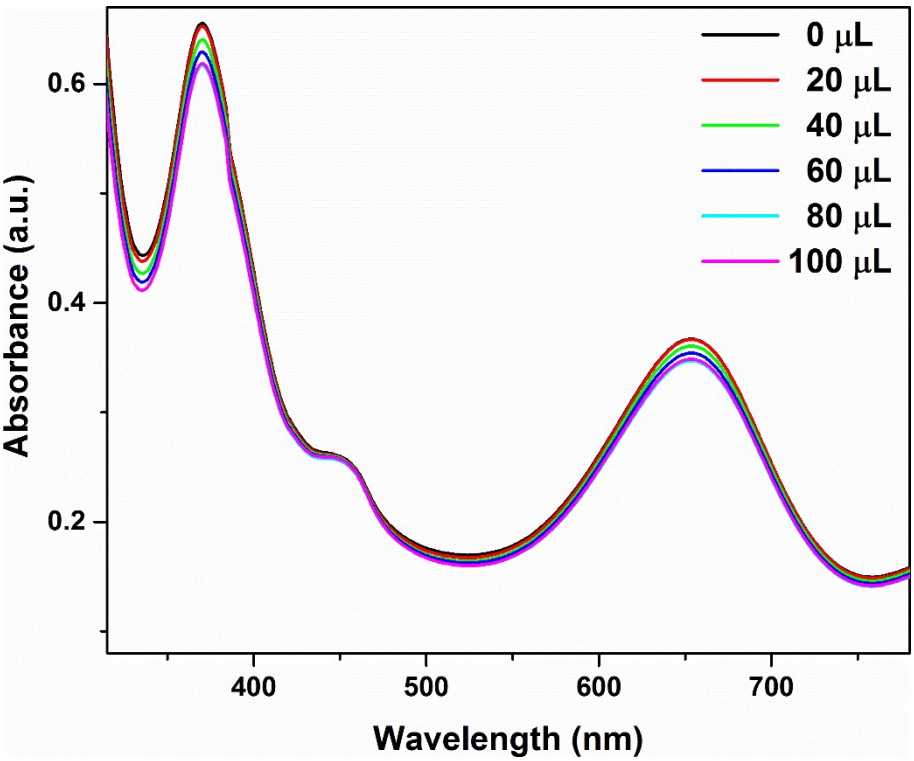

Figure S27. UV-vis absorption spectra of ox-TMB in presence of various concentrations of tryptophan.

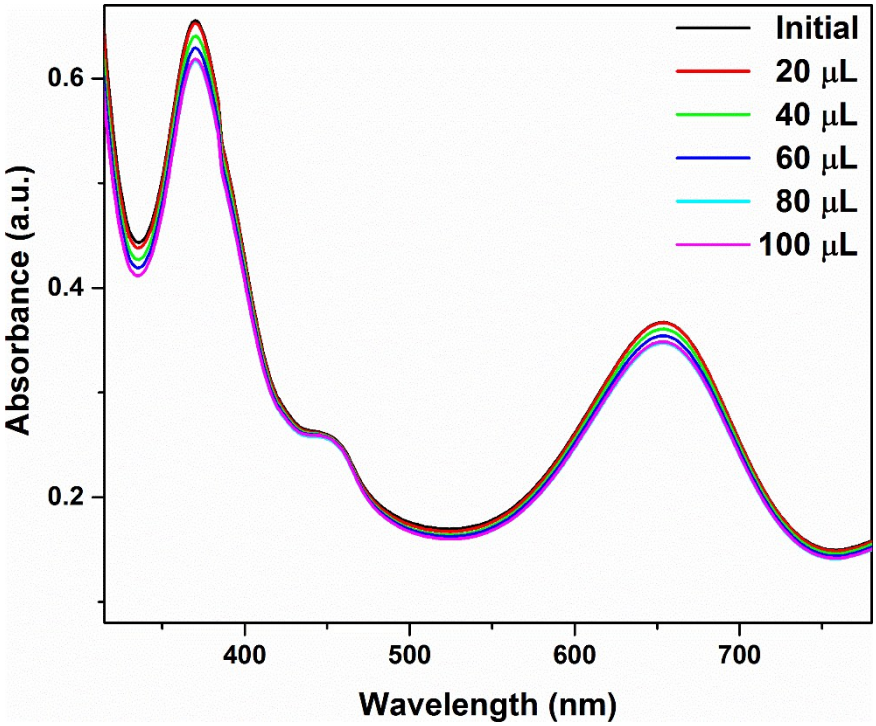

Figure S28. UV-vis absorption spectra of ox-TMB in presence of various concentrations of valine.

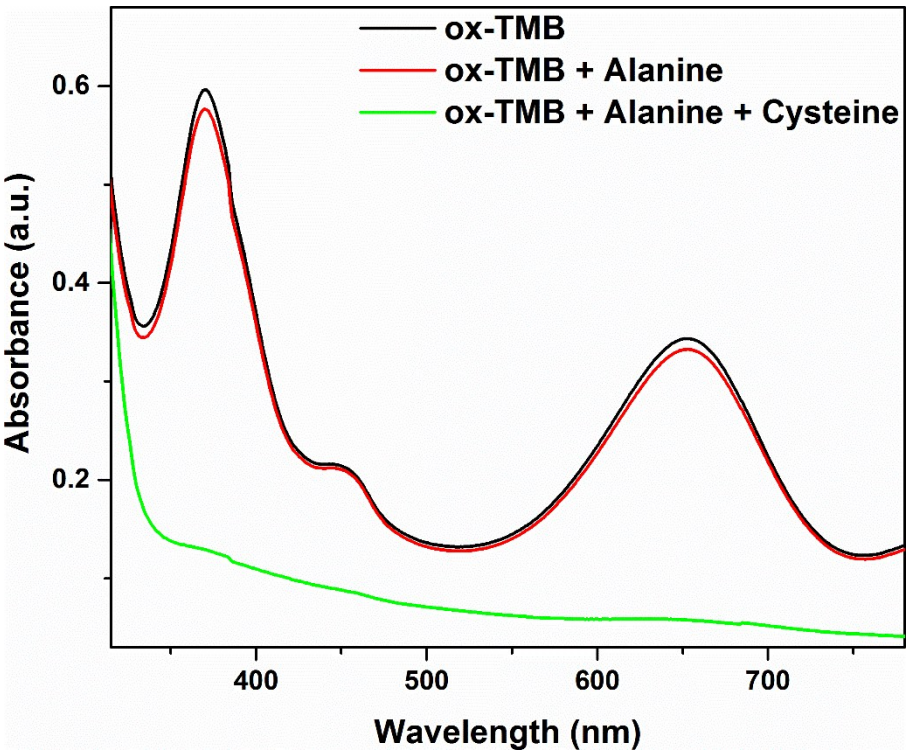

Figure S29. Change in the UV-vis absorption spectra of ox-TMB in presence of alanine, followed by the addition of cysteine.

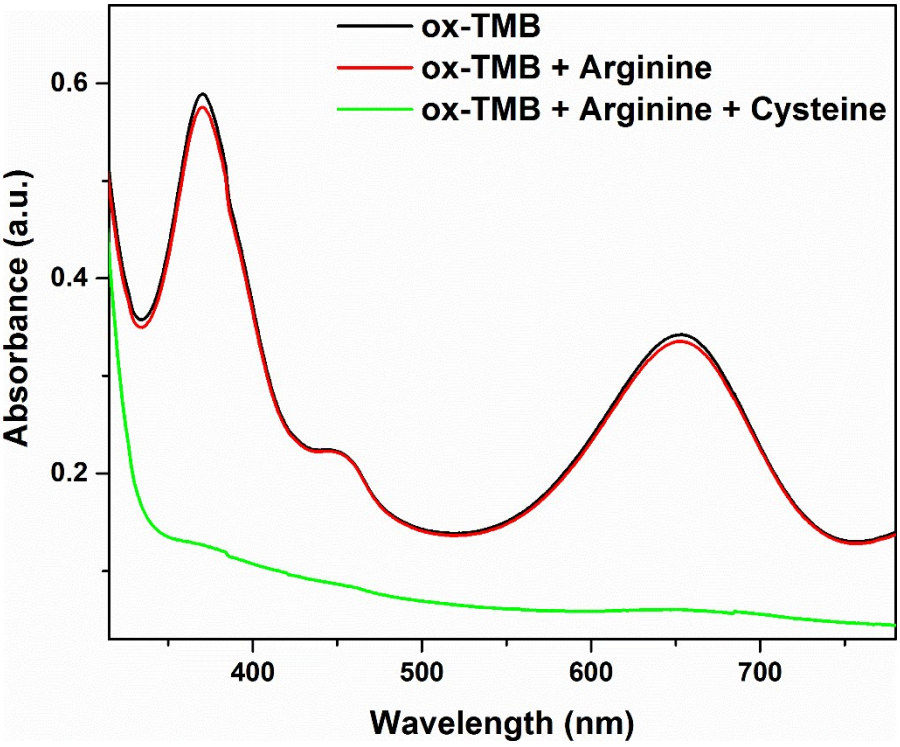

Figure S30. Change in the UV-vis absorption spectra of ox-TMB in presence of arginine, followed by the addition of cysteine.

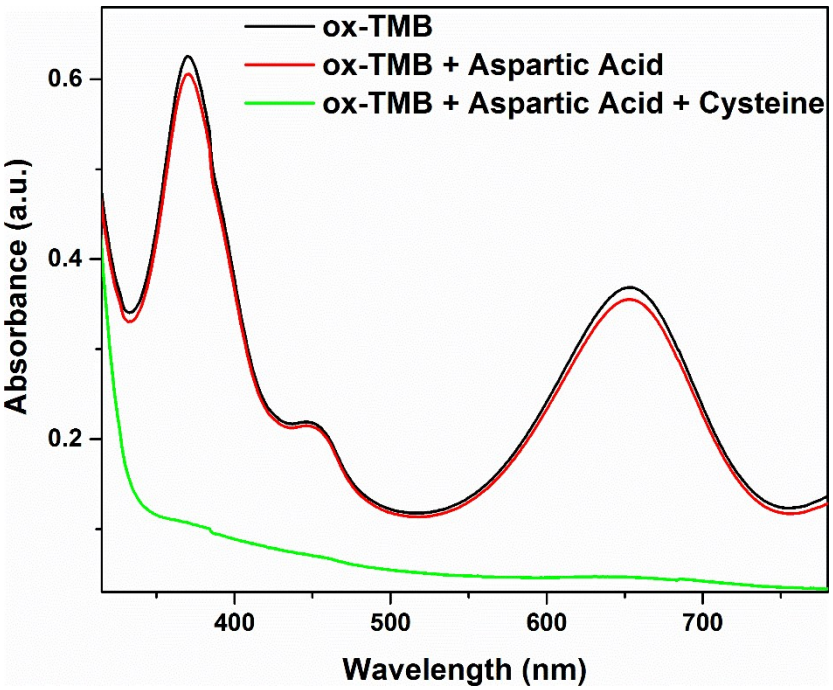

Figure S31. Change in the UV-vis absorption spectra of ox-TMB in presence of aspartic acid, followed by the addition of cysteine.

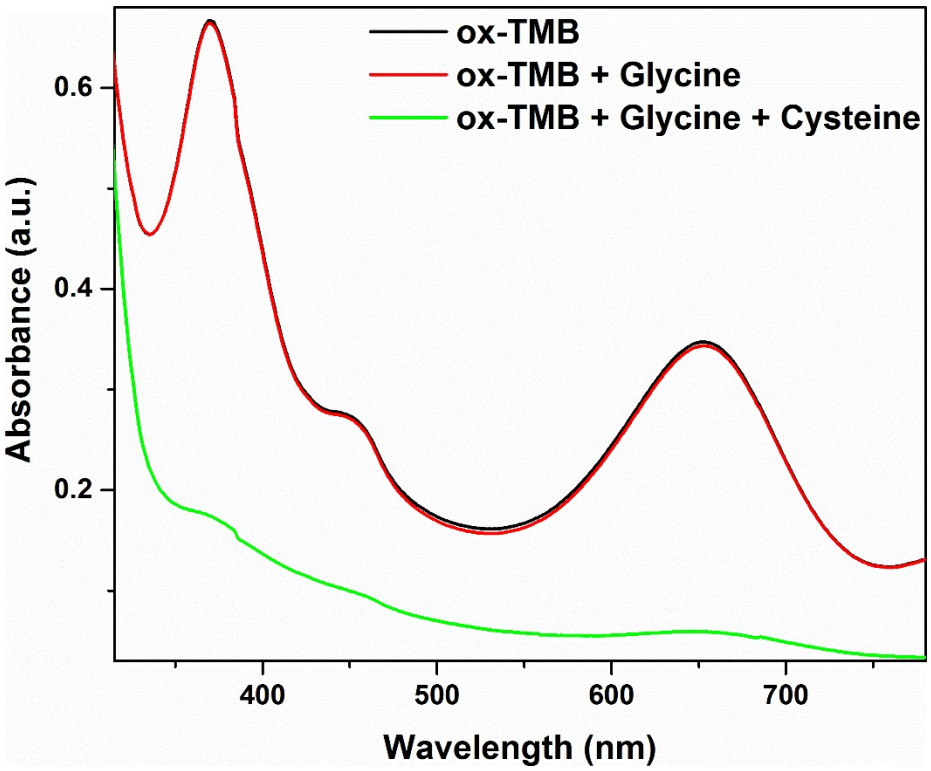

Figure S32. Change in the UV-vis absorption spectra of ox-TMB in presence of glycine, followed by the addition of cysteine.

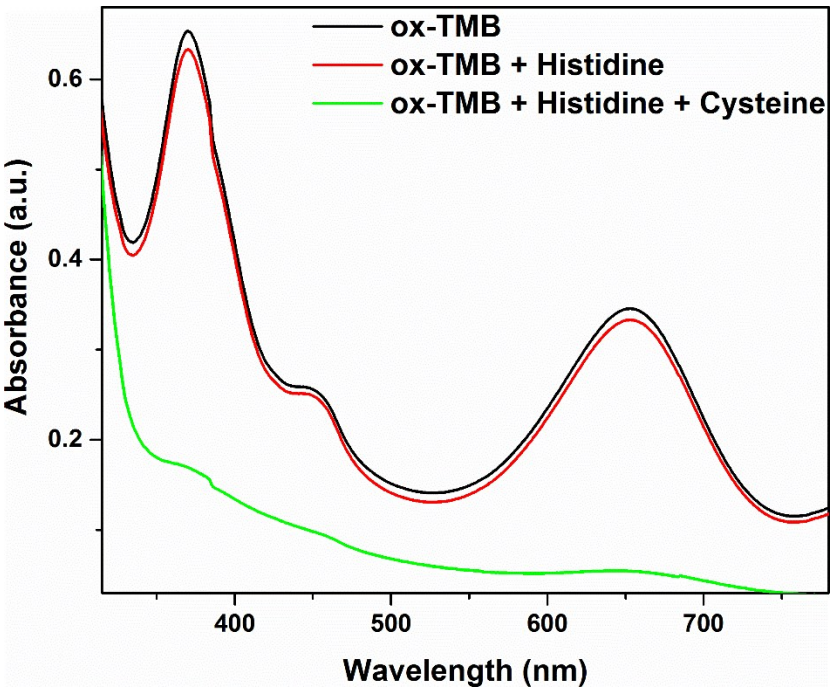

Figure S33. Change in the UV-vis absorption spectra of ox-TMB in presence of histidine, followed by the addition of cysteine.

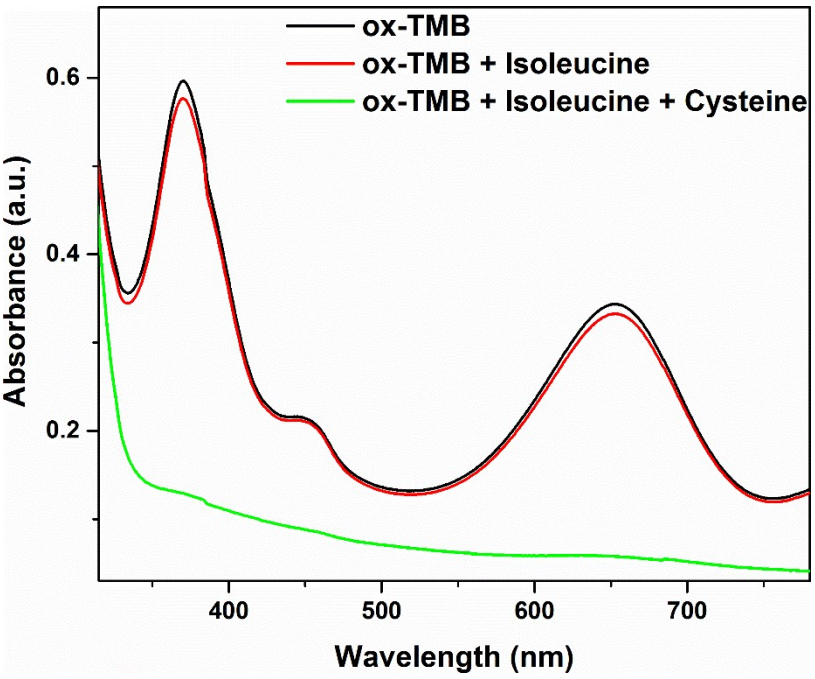

Figure S34. Change in the UV-vis absorption spectra of ox-TMB in presence of isoleucine, followed by the addition of cysteine.

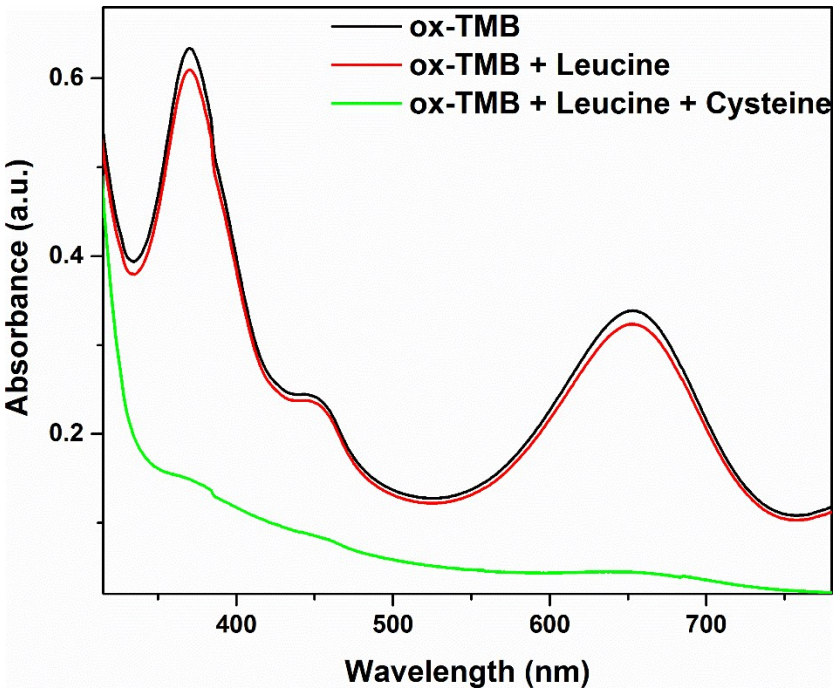

Figure S35. Change in the UV-vis absorption spectra of ox-TMB in presence of leucine, followed by the addition of cysteine.

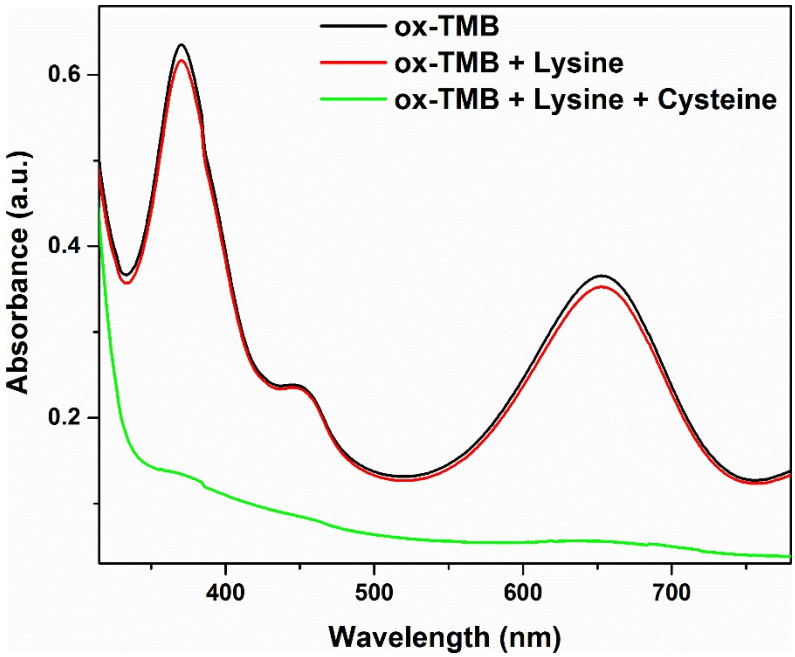

Figure S36. Change in the UV-vis absorption spectra of ox-TMB in presence of lysine, followed by the addition of cysteine.

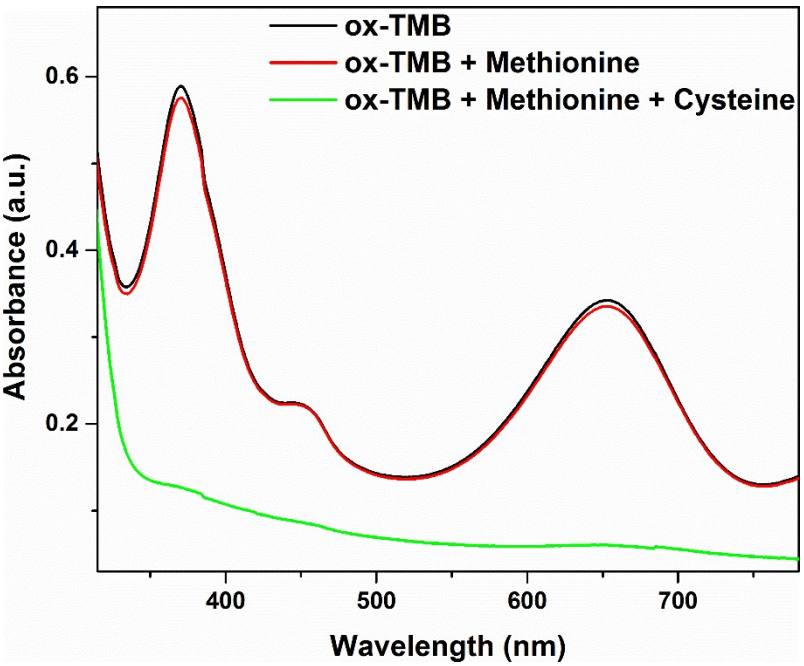

Figure S37. Change in the UV-vis absorption spectra of ox-TMB in presence of methionine, followed by the addition of cysteine.

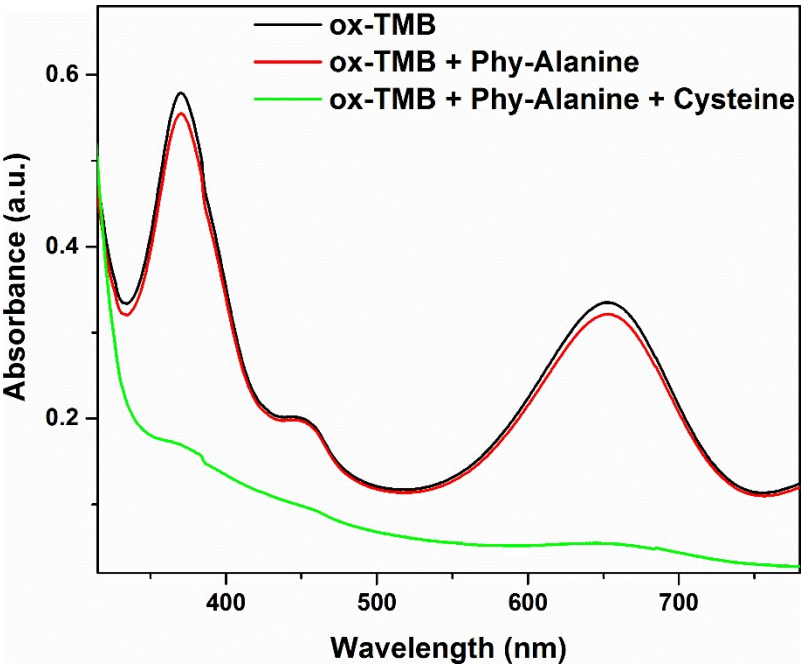

Figure S38. Change in the UV-vis absorption spectra of ox-TMB in presence of phenyl alanine, followed by the addition of cysteine.

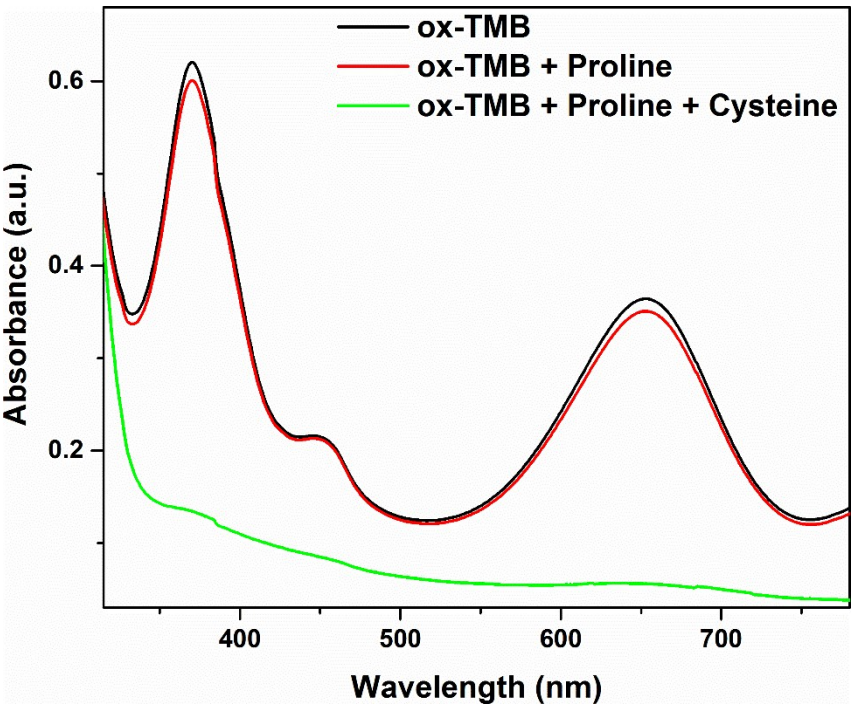

Figure S39. Change in the UV-vis absorption spectra of ox-TMB in presence of proline, followed by the addition of cysteine.

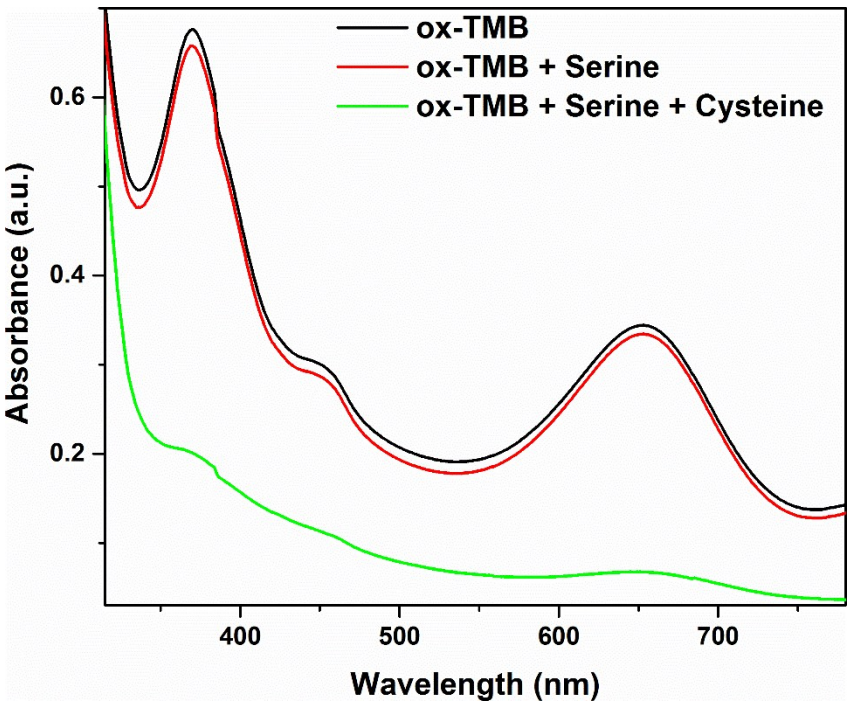

Figure S40. Change in the UV-vis absorption spectra of ox-TMB in presence of serine, followed by the addition of cysteine.

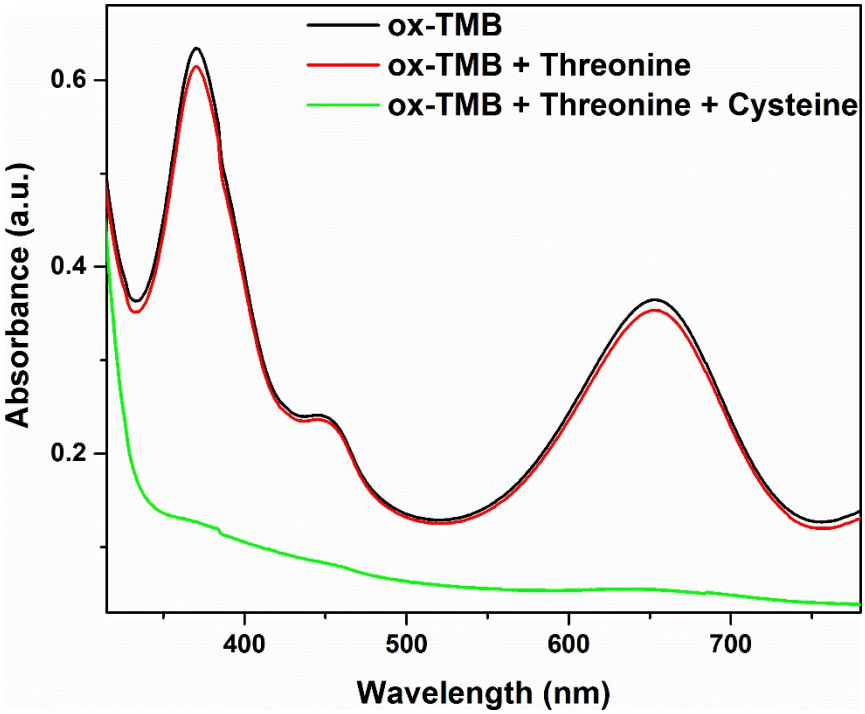

Figure S41. Change in the UV-vis absorption spectra of ox-TMB in presence of threonine, followed by the addition of cysteine.

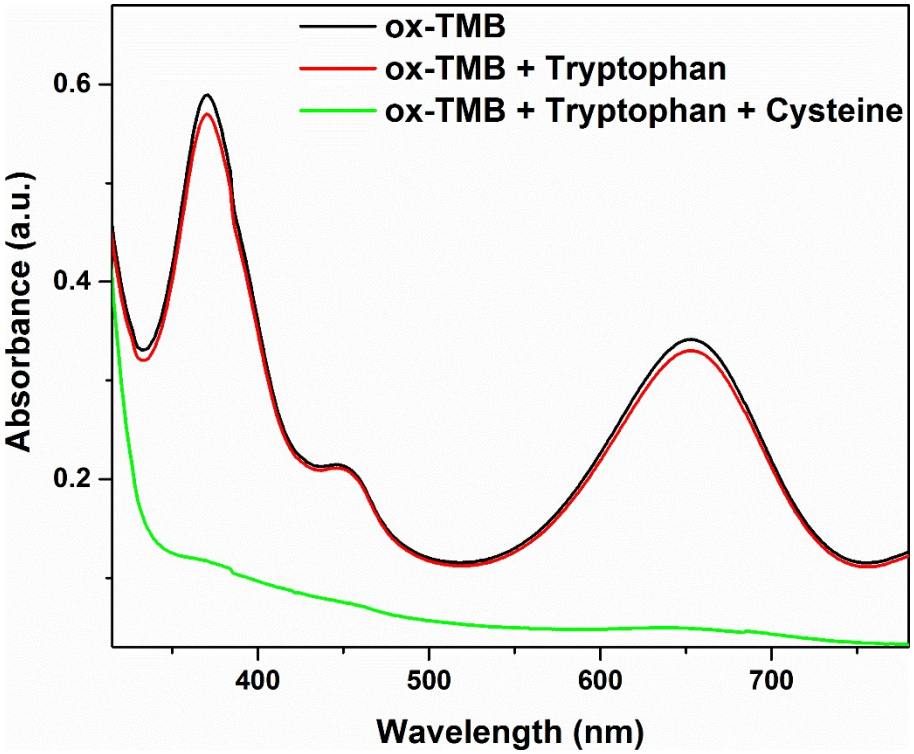

Figure S42. Change in the UV-vis absorption spectra of ox-TMB in presence of tryptophan, followed by the addition of cysteine.

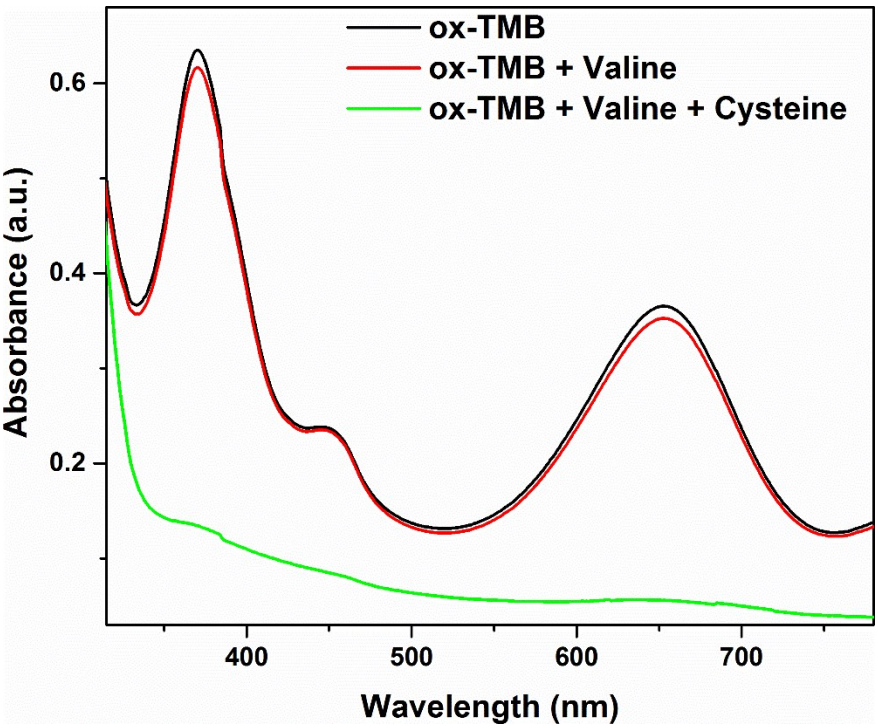

Figure S43. Change in the UV-vis absorption spectra of ox-TMB in presence of valine, followed by the addition of cysteine.

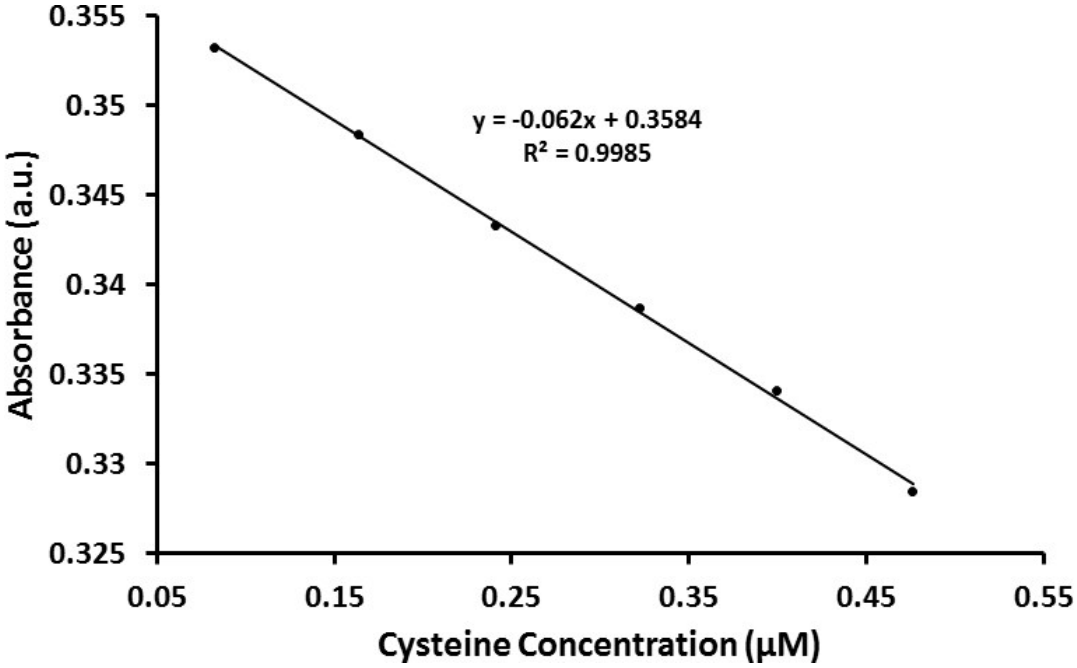

Figure S44. Change in the absorbance (monitored at λ_{max} = 652 nm) of ox-TMB as a function of cysteine concentration.

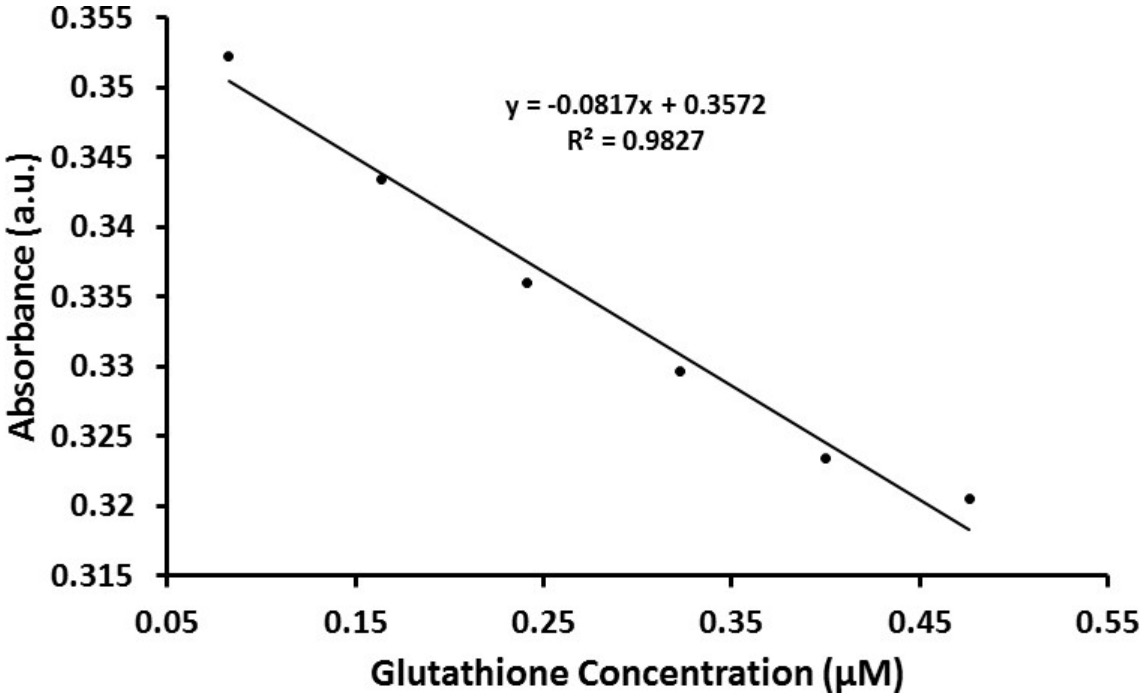

Figure S45. Change in the absorbance (monitored at λ_{max} = 652 nm) of ox-TMB as a function of glutathione concentration.

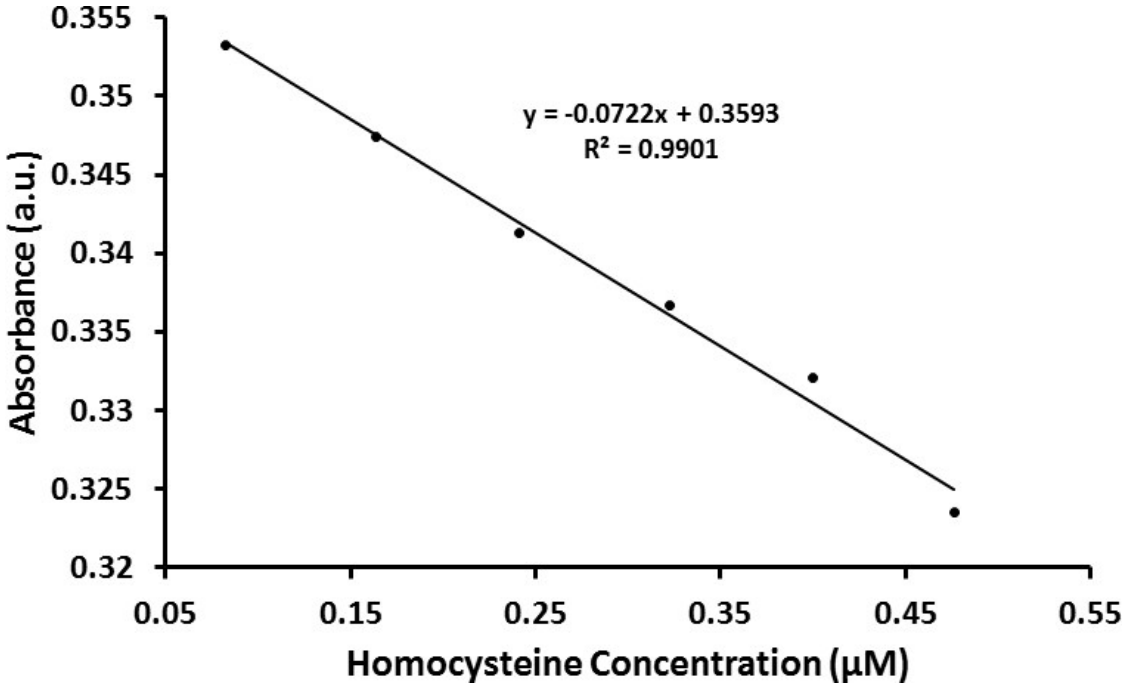

Figure S46. Change in the absorbance (monitored at λ_{max} = 652 nm) of ox-TMB as a function of homocysteine concentration.

Table S3. Comparison of the detection limits of different nano-enzymes (which mimic peroxidase/oxidase at pH = 4) towards biothiols.

Sl. No.	Nano-enzyme	Analytes	Dynamic range (μM)	Detection limit (μM)	Ref.
1.	Ce-DMTDC (**1'**)	Cys	0-1.0	0.150	This work
		Hcy		0.125	
		GSH		0.132	
2.	Fe-MIL-88-NH_2	Cys	1.0-80.0	0.390	[14]
		Hcy	1.0-80.0	0.400	
		GSH	1.0-100.0	0.450	
3.	Ce-MOF (MVCM)	Cys	0-40.0	0.139	[8]
		Hcy		0.143	
		GSH		0.129	
4.	photocatalytic UiO-66-NH_2	Cys	5.0-120.0	0.306	[15]
		Hcy		0.330	
		GSH		0.310	

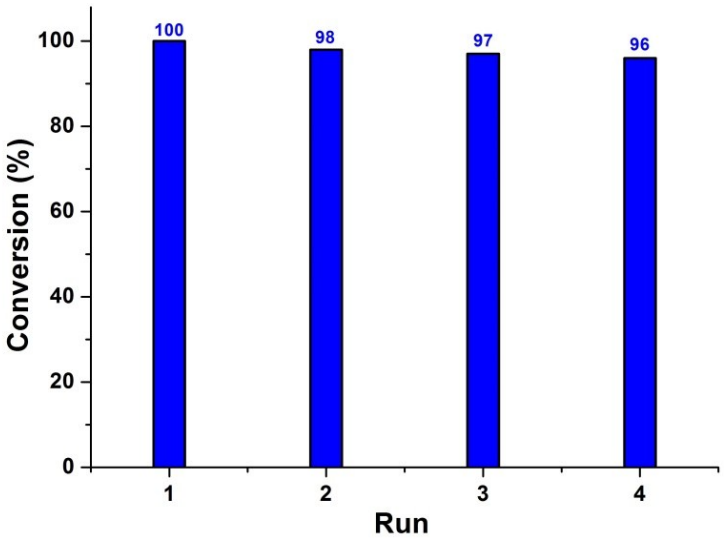

Figure S47. Reusability of **1′** for the aerobic oxidation of thiophenol under the optimized reaction conditions.

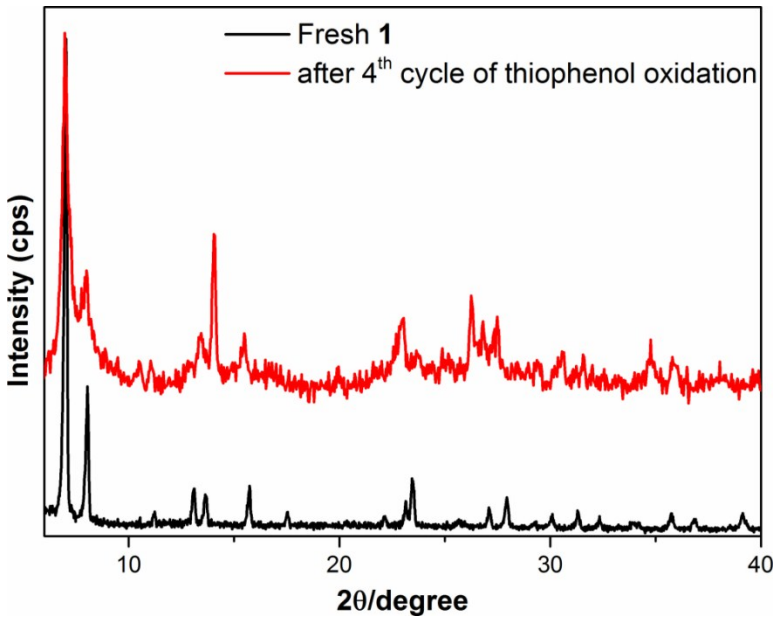

Figure S48. XRPD patterns of **1'** before and after catalytic oxidation of thiophenol.

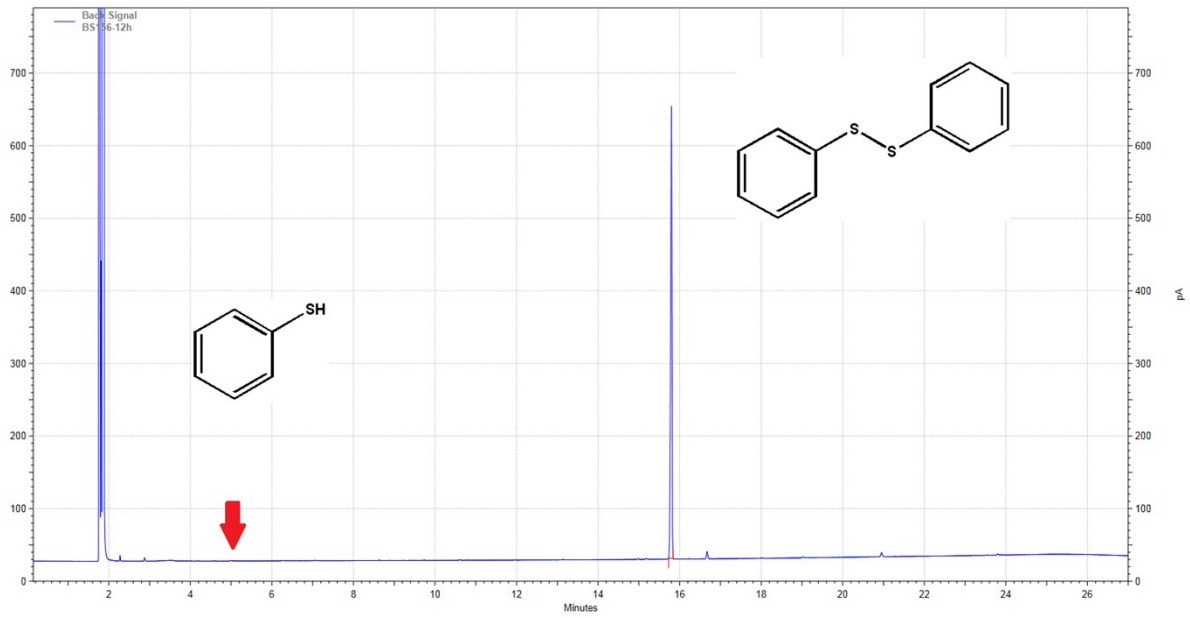

Figure S49. GC trace for the oxidation of thiophenol.

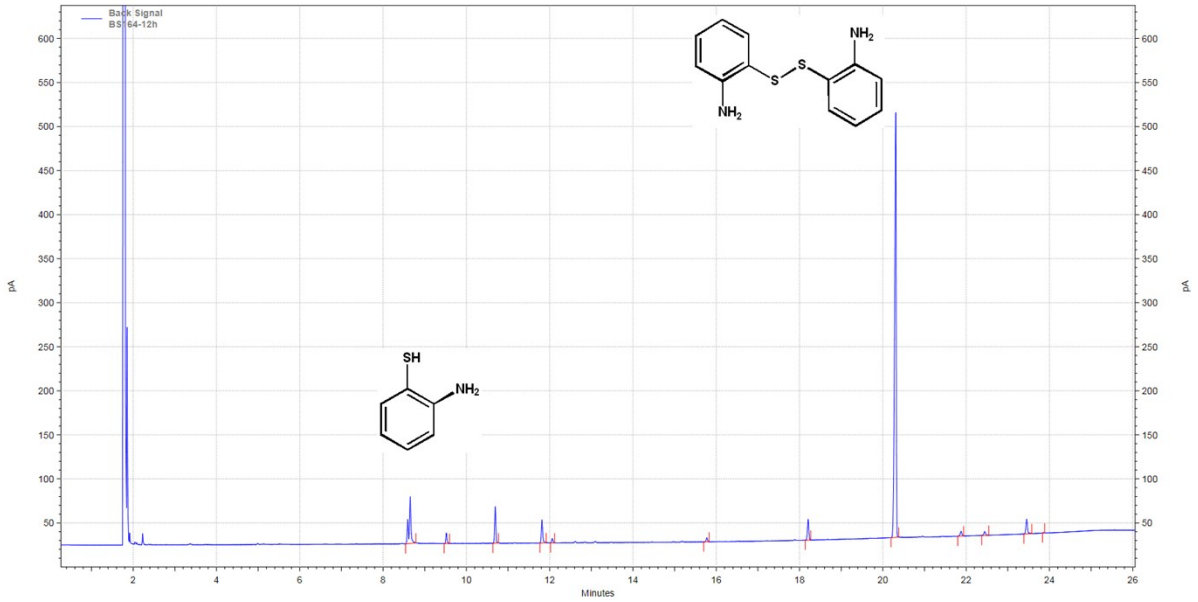

Figure S50. GC trace for the oxidation of 2-aminothiophenol.

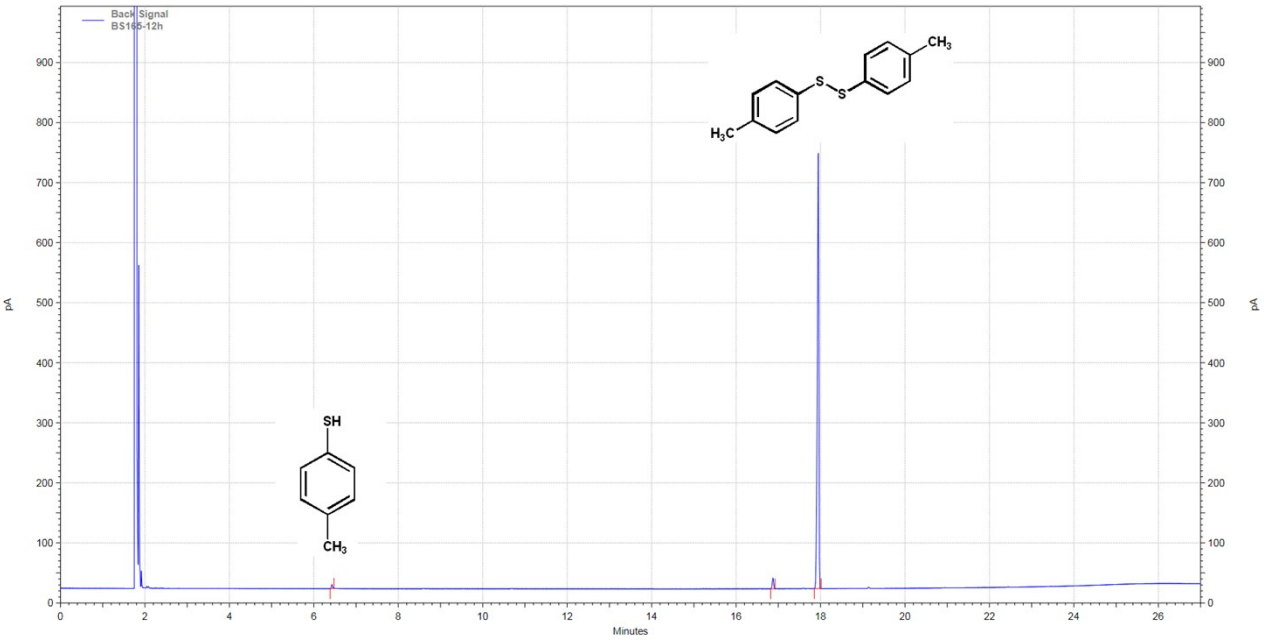

Figure S51. GC trace for the oxidation of 4-methylthiophenol.

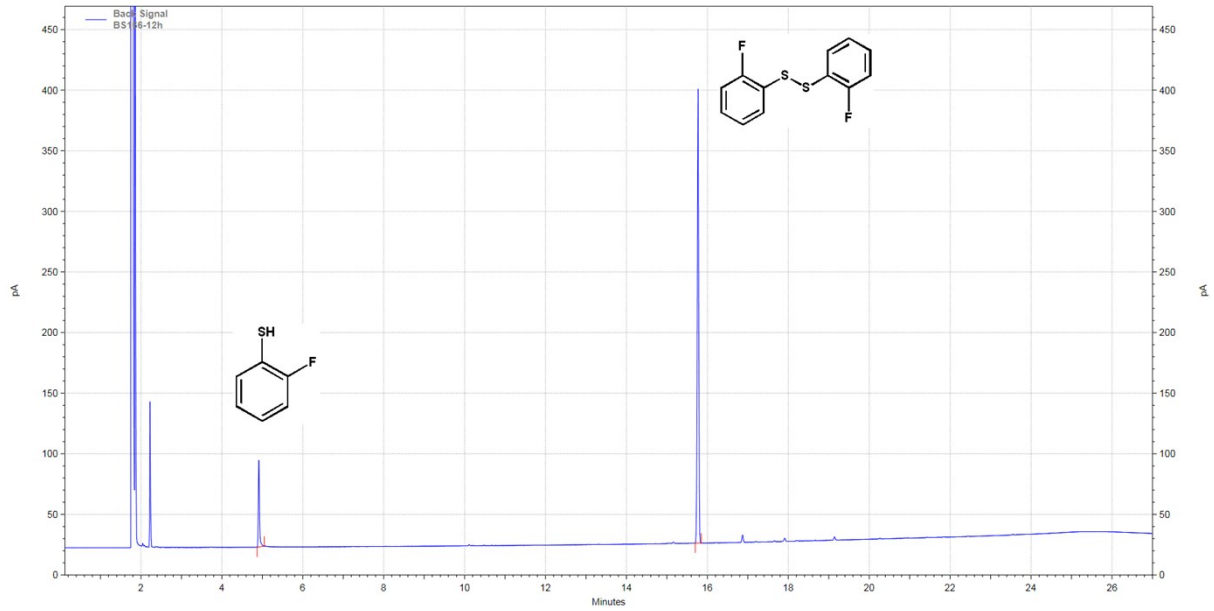

Figure S52. GC trace for the oxidation of 2-fluorothiophenol.

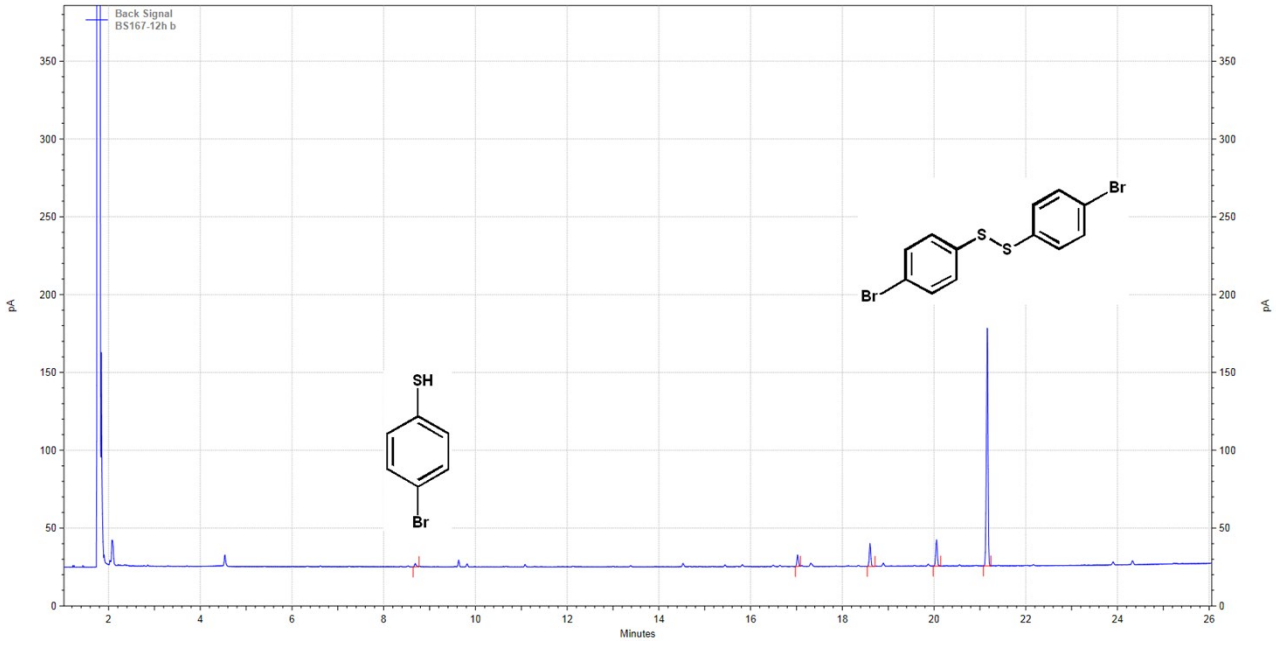

Figure S53. GC trace for the oxidation of 4-bromothiophenol.

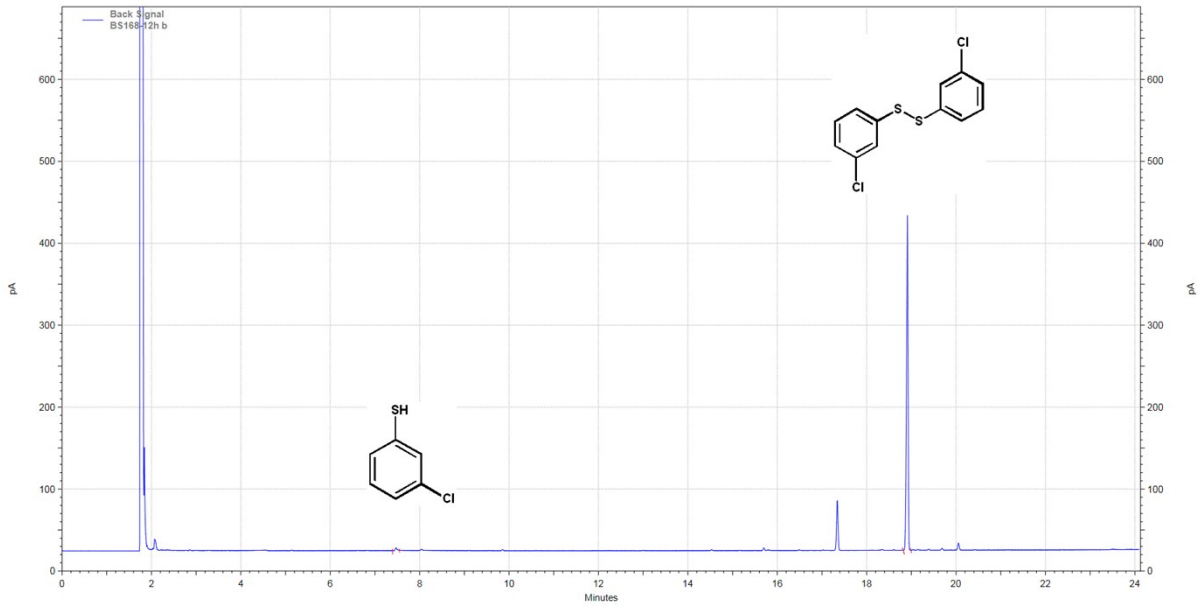

Figure S54. GC trace for the oxidation of 3-chlorothiophenol.

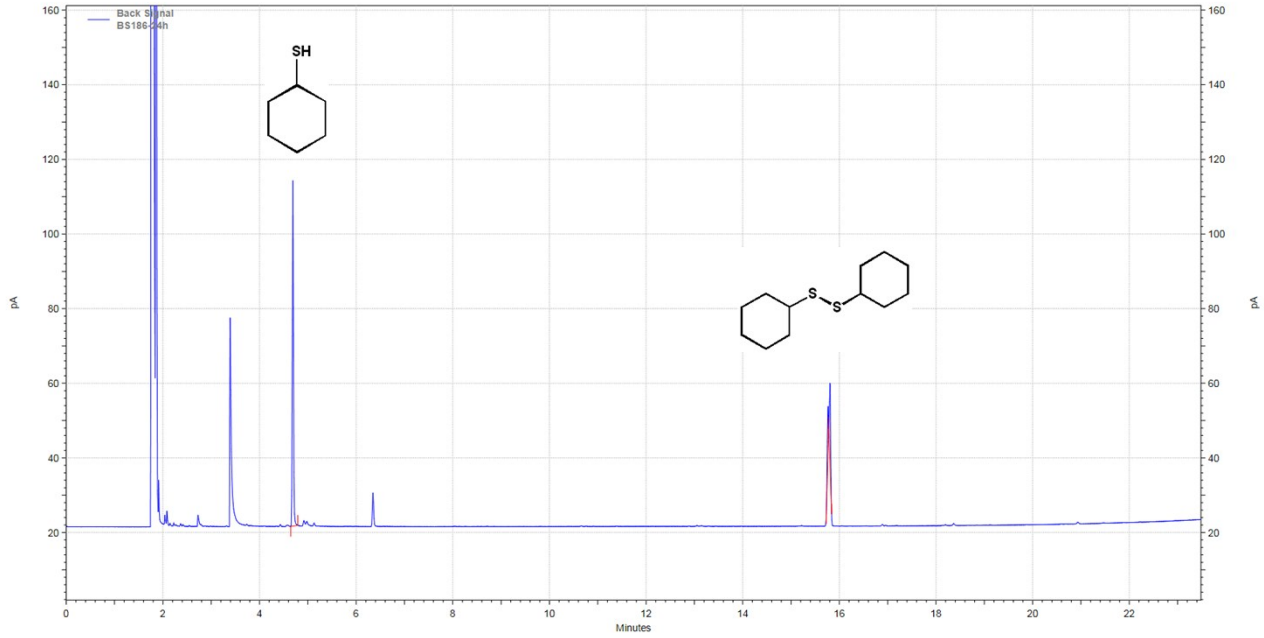

Figure S55. GC trace for the oxidation of cyclohexanethiol.

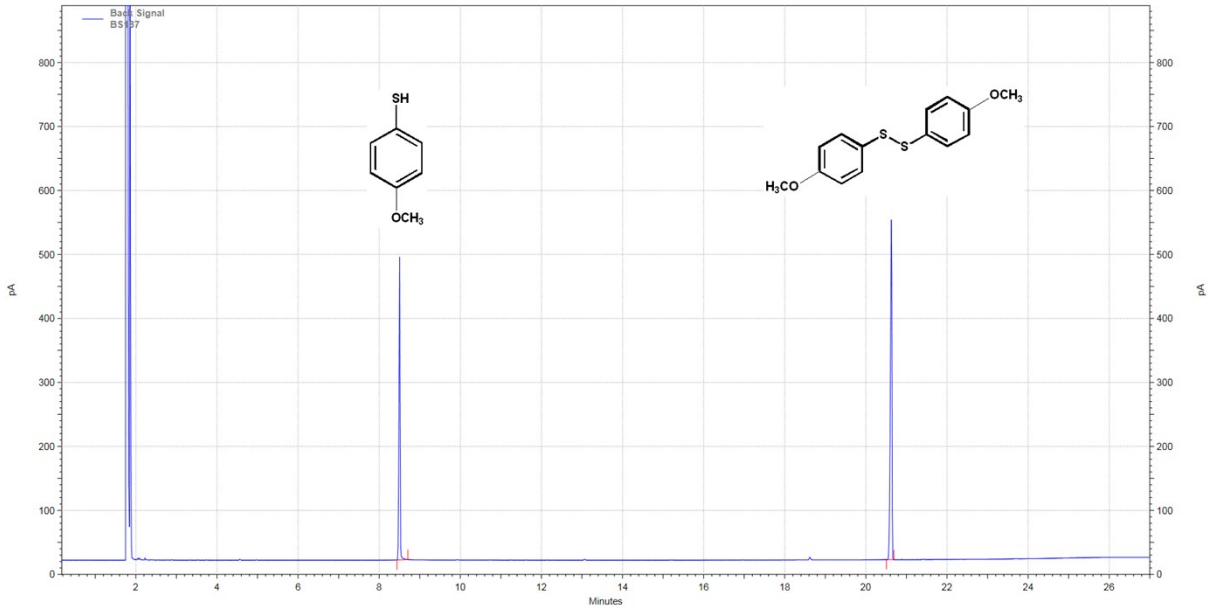

Figure S56. GC trace for the oxidation of 4-methoxythiophenol.

References:

[1] S. Mostakim, M. Grzywa, D. Volkmer and S. Biswas, *J. Solid State Chem.* **2015**, *232*, 221-227.
[2] K. Wang, H. Huang, W. Xue, D. Liu, X. Zhao, Y. Xiao, Z. Li, Q. Yang, L. Wang and C. Zhong, *CrystEngComm* **2015**, *17*, 3586-3590.
[3] J. Mu, L. Zhang, G. Zhao and Y. Wang, *Phys.Chem.Chem.Phys.* **2014**, *16*, 5709-15716.
[4] A. Asati, S. Santra, C. Kaittanis, S. Nath and J. M. Perez, *Angew. Chem. Int. Ed.* **2009**, *48*, 2308-2312.
[5] L. Ai, L. Li, C. Zhang, J. Fu and J. Jiang, *Chem. Eur. J.* **2013**, *19*, 15105-15108.
[6] C. Lu, X. Liu, Y. Li, F. Yu, L.Tang, Y. Hu and Y. Ying, *ACS Appl. Mater. Interfaces* **2015**, *7*, 15395−15402.
[7] Q. An, C. Sun, D. Li, K. Xu, J. Guo and C. Wang, *ACS Appl. Mater. Interfaces* **2013**, *5*, 13248−13257.
[8] Y. Xiong, S. Chen, F. Ye, L. Su, C. Zhang, S. Shen and S. Zhao, *Chem. Commun.* **2015**, *51*, 4635-4638.
[9] H. Tan, C. Ma, L. Gao, Q. Li, Y. Song, F. Xu, T. Wang and L. Wang, *Chem. Eur. J.* **2014**, *20*, 16377–16383.
[10] Y. L. Liu, X. J. Zhao, X. X. Yang and Y. F. Li, *Analyst* **2013**, *138*, 4526–4531.
[11] F.-X. Qin, S.-Y. Jia, F.-F. Wang, S.-H. Wu, J. Song and Y. Liu, *Catal. Sci. Tech.* **2013**, *3*, 2761-2768.
[12] W. Dong, X. Liu, W. Shi and Y. Huang, *RSC Adv.* **2015**, *5*, 17451-17457.
[13] D. Chen, B. Li, L. Jiang, D. Duan, Y. Li, J. Wang, J. He and Y. Zeng, *RSC Adv.* **2015**, *5*, 97910-97917.
[14] Z. Jiang, Y. Liu, X. Hua and Y. Li, *Anal. Methods* **2014**, *6*, 5647-5651.
[15] Z. Hua, X. Jianga, F. Xub, J. Jiac, Z. Longb and X. Houa, *Talanta* **2016**, *158*, 276–282.